Tanaka et al. Diagnostic Pathology 2012, 7:108
http://www.diagnosticpathology.org/content/7/1/108

DIAGNOSTIC PATHOLOGY

CASE REPORT Open Access

Pathological femoral fractures due to osteomalacia associated with adefovir dipivoxil treatment for hepatitis B: a case report

Motoyuki Tanaka[1], Takao Setoguchi[2*], Yasuhiro Ishidou[3], Yoshiya Arishima[1], Masataka Hirotsu[1], Yoshinobu Saitoh[1], Shunsuke Nakamura[1], Hironori Kakoi[1], Satoshi Nagano[1], Masahiro Yokouchi[1], Junichi Kamizono[1] and Setsuro Komiya[1]

Abstract

We present a case of a 62-year-old man who underwent total hip arthroplasty for treatment of pathologic femoral neck fracture associated with adefovir dipivoxil-induced osteomalacia. He had a 13-month history of bone pain involving his shoulders, hips, and knee. He received adefovir dipivoxil for treatment of lamivudine-resistant hepatitis B virus infection for 5 years before the occurrence of femoral neck fracture. Orthopedic surgeons should be aware of osteomalacia and pathological hip fracture caused by drug-induced renal dysfunction, which results in Fanconi's syndrome.

Virtual slides: The virtual slide(s) for this article can be found here: http://www.diagnosticpathology.diagnomx.eu/vs/1600344696739249

Keywords: Osteomalacia, Pathological femoral neck fracture, Adefovir dipivoxil, Hepatitis B, Fanconi's syndrome

Background

Hypophosphatemic osteomalacia caused by proximal renal tubule dysfunction induces Fanconi's syndrome, which leads to impaired reabsorption of amino acids, glucose, urate, and phosphate [1]. The chronic loss of phosphate and impaired synthesis of 1,25-dihydroxyvitamin D3 may lead to failure of bone mineralization. Recently, osteomalacia was reported in cases in which hepatitis B virus and human immunodeficiency virus (HIV) infections were treated using high-dose adefovir dipivoxil [2-6]. We report a case of a patient who underwent total hip arthroplasty for pathological femoral neck fracture associated with osteomalacia induced by low-dose adefovir dipivoxil treatment.

Case presentation

A 62-year-old man started experiencing pain in the right knee and left shoulder pain in January 2010. He visited a clinic and was administered salazosulfapyridine and methylprednisolone therapy for rheumatoid arthritis. However, the pain gradually increased, and he started experiencing pain in his hip joints as well. Therefore, he was admitted our hospital for further examination in February 2011. He had a 7-year history of chronic hepatitis caused by hepatitis B virus infection, and had received lamivudine therapy for 2 years. Because the virus developed resistance to lamivudine, he received adefovir dipivoxil for 5 years before the development of the femoral neck fracture. After adefovir dipivoxil treatment, his liver function was restored. Radiography showed femoral neck fractures (right, Garden III fracture; left, Garden IV fracture) and a distal right tibial fracture (Figure 1a) [7]. Magnetic resonance imaging (MRI) of both hip joints showed fractures across the right and left femoral neck and bone edema, which had low intensity on T1-weighted images and high intensity on T2-weighted images (Figure 1b). ^{99m}Tc-hydroxymethylene diphosphonate (HMDP) whole-body bone scintigraphy showed increased uptake of the radiotracer in the calvaria, maxilla, both scapulae, ribs, both femoral necks, right condyle of the femur, right tibia, and both tarsi (Figure 1c). He showed hypophosphatemia

* Correspondence: setoro@m2.kufm.kagoshima-u.ac.jp
[2]The Near-Future Locomotor Organ Medicine Creation Course (Kusunoki Kai), Graduate School of Medical and Dental Sciences, Kagoshima University, 8-35-1 Sakuragaoka, Kagoshima 890-8520, Japan
Full list of author information is available at the end of the article

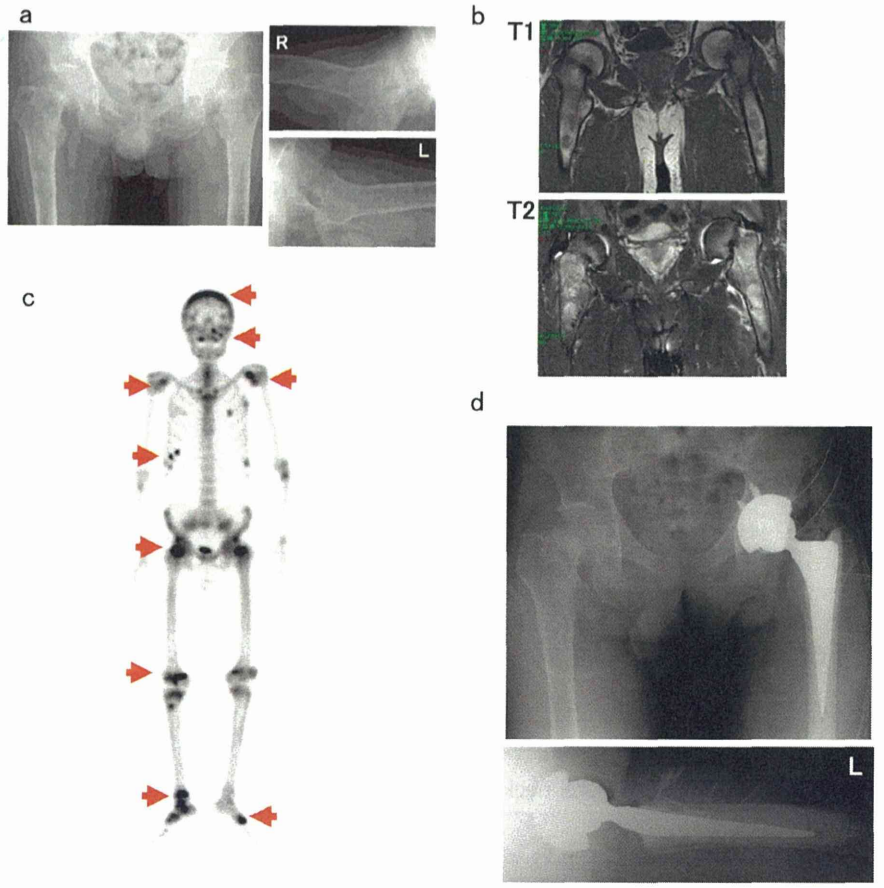

Figure 1 Imaging studies. a: Plain radiographs of both femurs reveal femoral neck fractures. (right, Garden III fracture; left, Garden IV fracture) **b**: Coronal T1-weighted image demonstrates low-intensity femoral neck fractures and the T2-weighted image shows high-intensity bone edema. **c**: ^{99m}Tc-hydroxymethylene diphosphonate (HMDP) scintigraphy demonstrates significant abnormal uptake in calvaria, maxilla, both scapulae, ribs, both femoral necks, right condyle of the femur, right tibia, and both tarsi. **d**: Plain radiographs of hip joints in which total hip arthroplasty was performed by inserting an implant in the left hip joint.

(2.0 mg/dL; normal range, 2.5–4.5 mg/dL) and increased levels of alkaline phosphatase (ALP, 1594 IU/L; normal range, 115–359 IU/L). Furthermore, he showed normal serum creatinine (0.7 mg/dL; normal range, 0.4–0.7 mg/dL), blood urea nitrogen (BUN, 12.3 mg/dL; normal range, 8.0–22.0 mg/dL), intact parathyroid hormone (PTH, 19 pg/mL; normal range, 10–65 pg/mL), and 1,25-dihydroxyvitamin D3 (40.0 pg/mL; normal range, 20–60 pg/mL) levels. Urinalysis revealed proteinuria. A 24-h study showed increased urinary excretion of phosphate (1004 mg/day; normal range, 70–220 mg/day), calcium (471.0 mg/day; normal range, 100–300 mg/day), *N*-acetylglucosaminidase (11.8 U/L; normal range, <7.0 U/L), and β2-microglobulin (64,579 μg/L; normal range, 230 μg/L). These findings indicated hypophosphatemia and hyperphosphaturia (increased levels of ALP). However, because the patient had normal levels of 1,25-dihydroxyvitamin D3, we considered that the impaired phosphate reabsorption could have been caused by dysfunction of the proximal renal tubule dysfunction and not by deficiency of vitamin D. Urinalysis and examination of urine samples collected over 24 h showed increased levels of *N*-acetylglucosaminidase and β2-microglobulin as well as phosphate wasting, which also indicated that these symptoms were caused by dysfunction of the proximal renal tubule.

On the basis of these findings, we made a diagnosis of osteomalacia and pathologic fractures due to Fanconi's syndrome secondary to adefovir therapy (10 mg/day). We conducted preoperative examinations to perform total hip arthroplasty. Prolonged bleeding time was observed by platelet aggregation failure and coagulation factor deficiency (Table 1). The coagulation disorder was suggested to have been caused by chronic hepatitis. The bleeding time was normalized by platelet transfusion. or double-labeling analysis, 1000 mg of tetracycline was orally

Table 1 Title: coagulation factors

	Activity	Normal range
Coagulation factor II	46.6%	(66.0–118.0)
Coagulation factor III	65.1%	(73.0–122.0)
Coagulation factor VII	65.6%	(54.0–162.0)
Coagulation factor VIII	89.8%	(78.0–165.0)
Coagulation factor IX	43.5%	(67.0–152.0)
Coagulation factor X	54.3%	(58.0–200.0)
Coagulation factor XI	43.5%	(75.0–137.0)
Von Willebrand factor	200%	(50.0–150.0)

administered at 10-day intervals. A 2-step procedure was performed under the same general anesthetic. During the first part of the procedure, biopsy of the iliac bone was performed, and during the second stage of the procedure, total hip arthroplasty was performed using a Zimmer implant (cemented collarless polished taper. stem, cementless trabecular metal modular acetabular cup, 36-mm head; Figure 1d). Because the acetabular roof bone was too fragile to support the acetabular components, bone fragment autografts prepared from the left femoral head were transplanted at the acetabular roof. The patient received intravenous antibiotics for 3 days. On the first postoperative day, the patient began rehabilitation under the supervision of a physiotherapist. He began using crutches for ambulation on postoperative day 7, with progressive weight-bearing as tolerated. The time to full weight-bearing was 3 weeks after the operation. The iliac bone and femoral head samples were fixed and stained using Villanueva bone stain and Villanueva–Goldner counterstain. The osteoid volume/mineralized bone volume ratio was 20.7% (average, <10%) and osteoid thickness was 25.1 μm (average, <12.5 μm; Figure 2a). Examination using tetracycline labeling showed no double-labeling pattern (Figure 2b) [8]. These findings confirmed that the pathological fractures were caused by osteomalacia (reviewed in [8]). After surgery, adefovir dipivoxil was switched with entecavir hydrate, and eldecalcitol and alendronate sodium hydrate were administered. These treatments normalized the blood phosphate level. The Japanese Orthopaedic Association Hip Score for the hip joints was 73 points at 2 months after surgery. He did not show any new pathological fractures.

Discussion

Adefovir dipivoxil is a commonly used antiviral agent in the treatment of chronic hepatitis B or HIV infection [9]. Fanconi's syndrome has been recognized as a

Figure 2 Pathological examinations. a: Mineralized bone tissues are colored in green and nonmineralized osteoid tissues are shown in orange by Villanueva-Goldner stain. Mineralized bone tissues are colored in purple and nonmineralized osteoid tissues are shown in the clear zone by Villanueva bone stain. The osteoids volume/mineralized bone volume ratio was 20.7% (normal range, less than 10%). Osteoid thickness was 25.1 μm (average, less than 12.5 μm). **b**: Tetracycline labeling examination showed no double-labeling pattern. These findings indicate mineralization deficiency and osteomalacia.

complication of high-dose adefovir dipivoxil therapy (dose, 60–120 mg/day) in the treatment of HIV infection [10]. Few studies have reported severe hypophosphatemia with 10 mg/day adefovir dipivoxil therapy [11-14]. In addition, to our knowledge, this is the first report of pathological femoral neck fracture associated with adefovir dipivoxil-induced osteomalacia treated by total hip arthroplasty. When orthopaedic surgeons encounter adefovir dipivoxil–treated chronic hepatitis B patients with pathological hip fractures, the patients' renal function and levels of electrolytes, including calcium and phosphorus, should be carefully monitored.

Fanconi's syndrome results from dysfunction of the proximal renal tubule, causing impaired reabsorption of amino acids, urate, bicarbonate, and phosphate and increased excretion of these solutes into the urine. The pathophysiology of proximal renal tubule dysfunction is thought to be an increase in the adefovir dipivoxil concentration in the mitochondria mediated by inhibition of several ATP-dependent transporters [15,16]. Patients with Fanconi's syndrome show low phosphate levels (because of renal phosphate loss) and normal levels of calcium, 25-hydroxyvitamin D, 1,25-dihydroxyvitamin D, and PTH and increased ALP levels. Radiography and bone scan showed multiple patterns of osteomalacia. Our findings were consistent with those in previous reports [17].

Entecavir is more effective than adefovir dipivoxil, with a favorable safety profile and low incidence of resistance [18]. We switched adefovir dipivoxil with entecavir hydrate as previously reported [19,20]. Entecavir may be a good treatment choice. In addition to adefovir dipivoxil, the patient received oral administration of lamivudine, rebamipide, rabeprazole sodium, and methylprednisolone. These drugs may have caused Fanconi's syndrome. After the patient's condition was diagnosed as Fanconi's syndrome, adefovir dipivoxil was replaced with entecavir hydrate. Thereafter, the symptoms of Fanconi's syndrome improved. These findings suggested that adefovir dipivoxil caused Fanconi's syndrome and osteomalacia.

In conclusion, orthopaedic surgeons should be aware of osteomalacia and pathologic fractures caused by adefovir dipivoxil administered as anti-hepatitis B virus therapy. In addition to the above-mentioned antiviral agent, ifosfamide, valproic acid, aminoglycosides, methyl-3-chromone, paraquat, L-lysine, calcineurin-inhibitor, or tetracycline may cause hypophosphatemic osteomalacia; therefore, serum ALP and phosphorus levels of patients receiving these drugs should be monitored [21-28].

Consent

Written informed consent was obtained from the patient and his family for publication of this case report. A copy of the written consent is available for review by the Editor-in-Chief of the journal.

Abbreviations

HIV: Human immunodeficiency virus; MRI: Magnetic resonance imaging; HMDP: ^{99m}Tc-hydroxymethylene diphosphonate; ALP: Alkaline phosphatase; BUN: Blood urea nitrogen; PTH: Parathyroid hormone.

Competing interests

The authors declare that they have no competing interests.

Authors' contributions

MT, YA, and SN were responsible for data collection. TS, YI, and SK, were responsible for literature search and manuscript preparation. MH, YS, and HK performed microscopic examinations, and JK performed surgery. All authors have read and approved the final manuscript.

Author details

[1]Department of Orthopaedic Surgery, Graduate School of Medical and Dental Sciences, Kagoshima University, Kagoshima, Japan. [2]The Near-Future Locomotor Organ Medicine Creation Course (Kusunoki Kai), Graduate School of Medical and Dental Sciences, Kagoshima University, 8-35-1 Sakuragaoka, Kagoshima 890-8520, Japan. [3]Department of Medical Joint Materials, Graduate School of Medical and Dental Sciences, Kagoshima University, Kagoshima, Japan.

Received: 30 May 2012 Accepted: 28 June 2012
Published: 20 August 2012

References

1. Clarke BL, Wynne AG, Wilson DM, Fitzpatrick LA: **Osteomalacia associated with adult Fanconi's syndrome: clinical and diagnostic features.** *Clin Endocrinol* 1995, **43**:479–490.
2. Verhelst D, Monge M, Meynard JL, Fouqueray B, Mougenot B, Girard PM, Ronco P, Rossert J: **Fanconi syndrome and renal failure induced by tenofovir: a first case report.** *Am J Kidney Dis* 2002, **40**:1331–1333.
3. Earle KE, Seneviratne T, Shaker J, Shoback D: **Fanconi's syndrome in HIV + adults: report of three cases and literature review.** *J Bone Miner Res* 2004, **19**:714–721.
4. Parsonage MJ, Wilkins EG, Snowden N, Issa BG, Savage MW: **The development of hypophosphataemic osteomalacia with myopathy in two patients with HIV infection receiving tenofovir therapy.** *HIV Med* 2005, **6**:341–346.
5. Zimmermann AE, Pizzoferrato T, Bedford J, Morris A, Hoffman R, Braden G: **Tenofovir-associated acute and chronic kidney disease: a case of multiple drug interactions.** *Clinical infectious diseases: an official publication of the Infectious Diseases Society of America* 2006, **42**:283–290.
6. Malik A, Abraham P, Malik N: **Acute renal failure and Fanconi syndrome in an AIDS patient on tenofovir treatment–case report and review of literature.** *J Infect* 2005, **51**:E61–E65.
7. Garden RS: **LOW-ANGLE FIXATION IN FRACTURES OF THE FEMORAL NECK.** *J Bone Joint Surg Br* 1961, **43-B**:647–663.
8. Ott SM: **Bone histomorphometry in renal osteodystrophy.** *Semin Nephrol* 2009, **29**:122–132.
9. Wong T, Girgis CM, Ngu MC, Chen RC, Emmett L, Archer KA, Seibel MJ: **Hypophosphatemic osteomalacia after low-dose adefovir dipivoxil therapy for hepatitis B.** *J Clin Endocrinol Metab* 2010, **95**:479–480.
10. Kahn J, Lagakos S, Wulfsohn M, Cherng D, Miller M, Cherrington J, Hardy D, Beall G, Cooper R, Murphy R, *et al*: **Efficacy and safety of adefovir dipivoxil with antiretroviral therapy: a randomized controlled trial.** *Jama* 1999, **282**:2305–2312.
11. Izzedine H, Kheder-Elfekih R, Housset P, Sarkozy C, Brocheriou I, Deray G: **Adefovir dipivoxil-induced acute tubular necrosis and Fanconi syndrome in a renal transplant patient.** *AIDS (London, England)* 2009, **23**:544–545.
12. Jung YK, Yeon JE, Choi JH, Kim CH, Jung ES, Kim JH, Park JJ, Kim JS, Bak YT, Byun KS: **Fanconi's syndrome associated with prolonged adefovir dipivoxil therapy in a hepatitis B virus patient.** *Gut and Liver* 2010, **4**:389–393.
13. Minemura M, Tokimitsu Y, Tajiri K, Nakayama Y, Kawai K, Kudo H, Hirano K, Atarashi Y, Yata Y, Yasumura S, *et al*: **Development of osteomalacia in a post-liver transplant patient receiving adefovir dipivoxil.** *World J Hepatol* 2010, **2**:442–446.
14. Lee HJ, Choi JW, Kim TN, Eun JR: **A case of severe hypophosphatemia related to adefovir dipivoxil treatment in a patient with liver cirrhosis**

related to hepatitis B virus. *The Korean Journal of Hepatology* 2008, **14**:381–386.
15. Tanji N, Tanji K, Kambham N, Markowitz GS, Bell A, D'Agati VD: **Adefovir nephrotoxicity: possible role of mitochondrial DNA depletion.** *Hum Pathol* 2001, **32**:734–740.
16. Cihlar T, Lin DC, Pritchard JB, Fuller MD, Mendel DB, Sweet DH: **The antiviral nucleotide analogs cidofovir and adefovir are novel substrates for human and rat renal organic anion transporter 1.** *Mol Pharmacol* 1999, **56**:570–580.
17. Izzedine H, Launay-Vacher V, Isnard-Bagnis C, Deray G: **Drug-induced Fanconi's syndrome.** *Am J Kidney Dis* 2003, **41**:292–309.
18. Asselah T, Lada O, Boyer N, Martinot M, Marcellin P: **Treatment of chronic hepatitis B.** *Gastroenterol Clin Biol* 2008, **32**:749–768.
19. Lai CL, Rosmawati M, Lao J, Van Vlierberghe H, Anderson FH, Thomas N, Dehertogh D: **Entecavir is superior to lamivudine in reducing hepatitis B virus DNA in patients with chronic hepatitis B infection.** *Gastroenterology* 2002, **123**:1831–1838.
20. Chang TT, Gish RG, Hadziyannis SJ, Cianciara J, Rizzetto M, Schiff ER, Pastore G, Bacon BR, Poynard T, Joshi S, *et al*: **A dose-ranging study of the efficacy and tolerability of entecavir in Lamivudine-refractory chronic hepatitis B patients.** *Gastroenterology* 2005, **129**:1198–1209.
21. Melnick JZ, Baum M, Thompson JR: **Aminoglycoside-induced Fanconi's syndrome.** *Am J Kidney Dis* 1994, **23**:118–122.
22. Yoshikawa H, Watanabe T, Abe T: **Fanconi syndrome caused by sodium valproate: report of three severely disabled children.** *Eur J Paediatr Neurol* 2002, **6**:165–167.
23. Otten J, Vis HL: **Acute reversible renal tubular dysfunction following intoxication with methyl-3-chromone.** *J Pediatr* 1968, **73**:422–425.
24. Vaziri ND, Ness RL, Fairshter RD, Smith WR, Rosen SM: **Nephrotoxicity of paraquat in man.** *Arch Intern Med* 1979, **139**:172–174.
25. Lo JC, Chertow GM, Rennke H, Seifter JL: **Fanconi's syndrome and tubulointerstitial nephritis in association with L-lysine ingestion.** *Am J Kidney Dis* 1996, **28**:614–617.
26. Varavithya W, Chulajata R, Ayudthya PS, Preeyasombat C: **Fanconi syndrome caused by degraded tetracycline.** *J Med Assoc Thail= Chotmaihet thangphaet* 1971, **54**:62–67.
27. Negro A, Regolisti G, Perazzoli F, Davoli S, Sani C, Rossi E: **Ifosfamide-induced renal Fanconi syndrome with associated nephrogenic diabetes insipidus in an adult patient.** *Nephrol Dial Transplant* 1998, **13**:1547–1549.
28. Morard I, Mentha G, Spahr L, Majno P, Hadengue A, Huber O, Morel P, Giostra E: **Long-term renal function after liver transplantation is related to calcineurin inhibitors blood levels.** *Clin Transplant* 2006, **20**:96–101.

doi:10.1186/1746-1596-7-108
Cite this article as: Tanaka *et al.*: Pathological femoral fractures due to osteomalacia associated with adefovir dipivoxil treatment for hepatitis B: a case report. *Diagnostic Pathology* 2012 **7**:108.

THE JOURNAL OF BIOLOGICAL CHEMISTRY VOL. 287, NO. 34, pp. 29101–29113, August 17, 2012

SnoN Suppresses Maturation of Chondrocytes by Mediating Signal Cross-talk between Transforming Growth Factor-β and Bone Morphogenetic Protein Pathways*[S]

Received for publication, February 2, 2012, and in revised form, June 21, 2012 Published, JBC Papers in Press, July 5, 2012, DOI 10.1074/jbc.M112.349415

Ichiro Kawamura[‡§], Shingo Maeda[‡1], Katsuyuki Imamura[‡§], Takao Setoguchi[¶], Masahiro Yokouchi[§], Yasuhiro Ishidou[‡], and Setsuro Komiya[‡§]

From the [‡]Department of Medical Joint Materials, [§]Department of Orthopedic Surgery, and the [¶]Near-Future Locomotor Organ Medicine Creation Course, Graduate School of Medical and Dental Sciences, 8-35-1 Sakuragaoka, Kagoshima University, Kagoshima 890-8544, Japan

Background: BMP signaling promotes chondrocyte maturation and, subsequently, endochondral ossification, whereas TGF-β signaling is inhibitory.
Results: TGF-β induced SnoN to suppress BMP signaling and chondrocyte hypertrophy.
Conclusion: SnoN mediates a signal cross-talk between TGF-β and BMP to regulate chondrocyte maturation.
Significance: Our data revealed an effector of TGF-β signaling as a putative therapeutic molecular target for cartilage/bone regeneration or osteoarthritis.

Hypertrophic maturation of chondrocytes is a crucial step in endochondral ossification, whereas abnormally accelerated differentiation of hypertrophic chondrocytes in articular cartilage is linked to pathogenesis of osteoarthritis. This cellular process is promoted or inhibited by bone morphogenetic protein (BMP) or transforming growth factor-β (TGF-β) signaling, respectively, suggesting that these signaling pathways cross-talk during chondrocyte maturation. Here, we demonstrated that expression of *Tgfb1* was increased, followed by phosphorylation of Smad2, during BMP-2-induced hypertrophic maturation of ATDC5 chondrocytes. Application of a TGF-β type I receptor inhibitor compound, SB431542, increased the expression of *Id1*, without affecting the phosphorylation status of Smad1/5/8, indicating that the activated endogenous TGF-β pathway inhibited BMP signaling downstream of the Smad activation step. We searched for TGF-β-inducible effectors that are able to inhibit BMP signaling in ATDC5 cells and identified SnoN. Overexpression of SnoN suppressed the activity of a BMP-responsive luciferase reporter in COS-7 cells as well as expression of *Id1* in ATDC5 cells and, subsequently, the expression of *Col10a1*, a hallmark of hypertrophic chondrocyte maturation. siRNA-mediated loss of SnoN showed opposite effects in BMP-treated ATDC5 cells. In adult mice, we found the highest level of *SnoN* expression in articular cartilage. Importantly, SnoN was expressed, in combination with phosphorylated Smad2/3, in prehypertrophic chondrocytes in the growth plate of mouse embryo bones and in chondrocytes around the ectopically existing hypertrophic chondrocytes of human osteoarthritis cartilage. Our results indicate that SnoN mediates a negative feedback mechanism evoked by TGF-β to inhibit BMP signaling and, subsequently, hypertrophic maturation of chondrocytes.

Bone formation is achieved by either intramembranous or endochondral ossification. The former process is characterized by differentiation of mesenchymal cells directly into bone-forming osteoblasts. Endochondral ossification is initiated by condensation of mesenchymal cells expressing a chondrogenic master regulator, *Sox9*, after which cells further differentiate into chondrocytes that are able to express a specific marker *Col2a1*, encoding type II collagen (1). Then the committed chondrocytes proliferate and convert into hypertrophic chondrocytes to eventually mineralize the surrounding cartilage matrix to be replaced by bone (2). Hypertrophic chondrocytes are characterized by a round large cell body and the ability to express *Col10a1*, encoding type X collagen. This hypertrophic conversion process is, at least in part, governed by Runx2 protein (*i.e.* Runx2 directly activates the promoter of *Col10a1* to promote chondrocyte hypertrophy) (3, 4). Mouse models in which dominant-negative Runx2 was overexpressed in chondrocytes showed suppressed chondrocyte hypertrophy, combined with complete loss of endochondral ossification (5). Conversely, forced expression of wild-type Runx2 in mouse chondrocytes resulted in accelerated differentiation of hypertrophic chondrocytes and bone formation (5, 6). Given that in permanent cartilage (*e.g.* normal articular cartilage on the joint space), chondrocytes do not undergo the late phase hypertrophic maturation, hypertrophic conversion of chondrocytes must be restricted to maintain a normal cartilage phenotype.

In addition to its indispensable role in physiological bone formation, the endochondral ossification process is a promising cellular event in the application of bone/cartilage regenerative medicine, which can be artificially engineered from human mesenchymal stem/stroma cells (7). Interestingly, these mesenchymal stem/stroma cells form bone trabeculae *in vivo* only

* This work was supported by Grants-in-Aid for Scientific Research (Scientific Research (C) (General)) 23592221 (to S. M.) and 23592222 (to Y. I.) and Japan Orthopedics and Traumatology Foundation, Inc., Grant 254.
[S] This article contains supplemental Table 1 and Fig. 1.
[1] To whom correspondence should be addressed. Tel.: 81-99-275-5381; Fax: 81-99-265-4699; E-mail: s-maeda@m3.kufm.kagoshima-u.ac.jp.

when they have developed hypertrophic structures *in vitro* before implantation (7), indicating that the efficiency of bone regeneration could be improved by promoting hypertrophic maturation of chondrocytes *in vitro*. In the case of cartilage regenerative medicine for treatment of cartilage defects, the maturation processes in engineered chondrocytes must be arrested because abnormally matured hypertrophic chondrocytes, expressing type X collagen, cause pathological conditions (*e.g.* osteoarthritis (OA)[2]) (8–10). *In vitro*, mesenchymal stem/stroma cells rapidly express *COL10A1* in monolayer or pellet culture before the cells demonstrate morphology of hypertrophic chondrocytes, a phenomenon that is a major problem of cartilage tissue engineering (11, 12), suggesting that the mechanism by which mesenchymal stem/stroma cells induce type X collagen is different from that in growth plate chondrocytes. Importantly, it is largely unknown how the expression of type X collagen is induced in degenerating articular chondrocytes.

Both BMP and TGF-β signaling promote early chondrogenesis. Members of the TGF-β family, including BMPs, transduce signals through type II and type I receptors to activate receptor-regulated Smads (R-Smads). Upon ligand binding, TGF-β type I receptors activate Smad2/3, whereas BMP type I receptors phosphorylate Smad1/5/8 in the cytoplasm. After forming a trimeric complex with Smad4 (co-Smad), R-Smads translocate into the nucleus to directly or indirectly regulate the transcription of target genes (13). Forced expression of an extracellular BMP-antagonist, Noggin (*Nog*), in chondrocytes *in vivo* showed no cartilage formation in transgenic mice (14). Similarly, cartilage-specific combined loss of BMP type I receptors (*Bmpr1a* and *Bmpr1b*) or double deletions of BMP-type R-Smads (*Smad1* and *Smad5*) showed severely impaired chondrogenesis in mice (15, 16). These mouse models clearly demonstrated the critical roles of the BMP-Smad pathway in early chondrogenesis. TGF-β signaling promotes the early stage of chondrogenesis by enabling Smad3 to form an active transcriptional complex with CEBP/p300 and Sox9 (17). However, at the late maturation stage, BMP and TGF-β signaling show mutually opposite roles in chondrocyte hypertrophy. BMP signaling directly accelerates the expression of *Col10a1* in concert with Runx2 (18–20), whereas the chondrocyte-specific expression of constitutively active *Bmpr1a* promoted the maturation and hypertrophy of chondrocytes in transgenic mice (21). An intra-articular injection of BMP-2 in mice accelerated cartilage chondrocyte hypertrophy and endochondral ossification to form osteophytes, a phenotype of OA (22). In contrast, loss of TGF-β signaling in the cartilage of mice, achieved by targeted ablation of the *Smad3* gene or forced expression of the dominant negative TGF-β type II receptor, resulted in accelerated differentiation of chondrocytes into hypertrophy coupled with an OA-like destruction of cartilage (23, 24). Similarly, chondrocyte-specific transgenic mice of Smurf2, an E3 ubiquitin ligase of the negative regulator for TGF-β signaling, also showed an OA-like change in articular cartilage with ectopic hypertrophic chondrocytes (25). These mouse models indicated an indispensable role of TGF-β signaling in preventing chondrocyte hypertrophy in articular cartilage, although the underlying molecular mechanisms are unclear. Interestingly, Smad3-deficient chondrocytes showed enhanced BMP signaling and accelerated hypertrophic differentiation *in vitro*, suggesting a role of endogenous TGF-β signaling in suppressing BMP signaling during chondrocyte maturation (26). Taken together, promoting TGF-β signaling in maturing chondrocytes is a promising candidate approach to manipulate the differentiation to fine tune chondrocyte hypertrophy. However, because TGF-β signaling regulates a wide range of pivotal biological functions (*e.g.* cell growth, differentiation, motility, extracellular matrix production, and apoptosis) in various target cells, blocking of the entire TGF-β signaling pathway might result in undesirable side effects. Therefore, to eliminate these problems, the direct mediator(s) induced by TGF-β signaling to inhibit BMP signaling in maturing chondrocytes should be an appropriate molecular target. Here, we show that SnoN is as a spatial and temporal effector of TGF-β signaling to inhibit the BMP-Smad pathway and, subsequently, chondrocyte hypertrophy.

EXPERIMENTAL PROCEDURES

Cell Culture—The chondrogenic cell line ATDC5 was obtained from RIKEN BioResource Center. The cells were maintained in Dulbecco's modified Eagle's medium (DMEM)/Ham's F-12 (1:1) (Invitrogen) containing 5% fetal bovine serum (FBS) and 100 units/ml penicillin G and 100 μg/ml streptomycin. Differentiation of ATDC5 cells was induced in serum-free medium containing insulin/transferrin/selenium supplement (Sigma) on collagen type I-coated culture plates (Iwaki). For expression analysis of differentiation markers in ATDC5 cells, micromass culture was performed as previously described (27), to accelerate maturation of chondrocyte differentiation. A monolayer culture system was employed for analysis of phosphorylation of Smads by immunoblotting because the cell lysis of micromass culture for cytoplasmic/nuclear protein was less efficient, and in addition, these experiments were not intended to evaluate the chondrogenic differentiation of early time points but rather the intracellular signaling. Monolayer culture was also performed for immunocytochemistry because of the difficulty in identifying individual cells in the micromass culture. Primary chondrocytes were harvested from 4-day-old mice of C57BL/6J background as described (28). Primary chondrocytes were induced to differentiate in a monolayer culture. COS-7 cells were purchased from the RIKEN BioResource Center and maintained in DMEM supplemented with 10% FBS and antibiotics.

Ligands and Inhibitors—BMP-2 (Peprotech) was applied at a concentration of 300 ng/ml, whereas TGF-β1 (Peprotech) was used at 5 ng/ml. The day of the first ligand application was referred to as day 0. SB431542 (Sigma) was applied at 1 μM for 30 min prior to ligand stimulation, and DMSO was used as a mock control. When indicated, cells were treated with a proteasome inhibitor, MG132 (Merck), at 10 μM 12 h prior to cell lysis.

Bone Organ Culture—Metatarsal bone rudiments were harvested from C57BL/6J embryos at 17.5 days postcoitum (E17.5) and cultured in DMEM supplemented with 10% FBS, 100

[2] The abbreviations used are: OA, osteoarthritis; BMP, bone morphogenetic protein; qPCR, quantitative PCR; E17.5, embryonic day 17.5.

units/ml penicillin G, and 100 μg/ml streptomycin, as described (29). Cultured bones were stained with Alcian blue and alizarin red dyes according to a standard protocol for skeletal preparation. Briefly, bones fixed in 96% ethanol were stained with 0.015% Alcian blue 8GX (Sigma) in a mixture solution of 96% ethanol, acetic acid (4:1) for 1 day, followed by a dehydration step in 100% ethanol. Dehydrated bones were immersed briefly in 1% potassium hydroxide (KOH), followed by staining in 0.001% alizarin red S (Sigma) in 1% KOH for 1 day. Images were analyzed using ImageJ software (National Institutes of Health). Animal experiments were approved by the Institutional Animal Care and Use Committee of Kagoshima University (MD11019).

RNA Interference—Dharmacon siRNA ON-TARGETplus SMARTpool, a mixture of four independent siRNAs of mouse SnoN (*Skil*), and the control reagent were purchased from Thermo Scientific. siRNA was transfected into cells using Lipofectamine RNAiMax (Invitrogen). Ligands and SB431542 were added to the culture simultaneously after an overnight transfection of siRNA.

Plasmids—9xCAGA luc, BRE luc, ALK5TD, ALK3QD, and FLAG-tagged human SnoN in pcDEF3 were kind gifts from Dr. Kohei Miyazono (University of Tokyo). pGL4.75hRlucCMV was purchased from Promega. cDNA of mouse SnoN was cloned from ATDC5 by employing a reverse transcription-polymerase chain reaction (RT-PCR)-based technique, subcloned into the entry vector, pENTR, and further transferred into pEF-DEST51 by attL-attR (LR) recombination (Invitrogen).

Lentivirus—pENTR-SnoN and pENTR-5′EF1αP were subjected to LR recombination with pLenti6.4/R4R2/V5-DEST (Invitrogen) to generate a lentiviral vector, which expresses C-terminal V5-tagged *SnoN* from the EF1α promoter. The lentiviral expression vector or pLenti6/V5/GW-lacZ control vector was transfected into 293FT cells to generate lentivirus. The conditioned medium containing lentivirus was incubated with mouse metatarsal bones for 16 h for infection. The infection efficiency was monitored by immunohistochemistry on the coronal section of infected bones using anti-V5-FITC antibody.

Immunoblotting—Cells were lysed in either M-PER lysis buffer (Thermo Scientific) supplemented with aprotinin, sodium orthovanadate, and phenylmethylsulfonyl fluoride (PMSF) or directly with 1× SDS sample buffer. SDS-PAGE, membrane transfer, and chemiluminescence were performed by using a standard protocol. Blots were incubated with anti-SnoN (1:200, H-317, sc-9142, Santa Cruz Biotechnology, Inc. (Santa Cruz, CA)), anti-phospho-Smad1/5/8 (1:1000, catalog no. 9511), anti-phospho-Smad2 (1:1000, catalog no. 3108), anti-Smad1 (1:1000, catalog no. 9743), horseradish peroxidase (HRP)-conjugated anti-rabbit secondary antibody and anti-mouse secondary antibody (1:10,000) (Cell Signaling), anti-Smad2/3 (1:1000, catalog no. 610842, BD Biosciences), anti-tubulin (1:1000, DM1A, T9026, Sigma), and anti-Mmp13 (1:1000, ab58836, Abcam). Signals were detected using the LAS 4000 mini image analyzer (Fujifilm).

Immunocytochemistry and Immunohistochemistry—For immunocytochemistry, cells were fixed with 4% paraformaldehyde in PBS for 30 min and treated with 0.2% Triton X-100. For antigen retrieval of type X collagen, cells were digested with 5 units/ml hyaluronidase (Calbiochem) for 30 min at 37 °C, followed by pepsin (Quartett) digestion for 15 min at 37 °C. CAS block (Zymed Laboratories Inc.) was used for blocking. Cells were incubated with anti-type X collagen (1:50, LB-0092, LSL), anti-SnoN (1:50, H-317, sc-9142, Santa Cruz Biotechnology, Inc.), anti-phospho-Smad2 (1:100, catalog no. 3108, Cell Signaling), and anti-Smad2/3 (1:100, catalog no. 610842, BD Biosciences). Anti-rabbit Alexa Fluor 488 (1:200, A11008), or anti-mouse Alexa Fluor 546 (1:200, A11060) (Invitrogen) was used to detect signals. Normal rabbit or mouse serum was used as negative control. For immunohistochemistry, we obtained human samples from individuals undergoing total hip arthroplasty after obtaining written informed consent as approved by the Ethics Committee of Kagoshima University (number 22-85). Formalin-fixed human femoral heads, mouse E17.5 embryo humeri, or bone organ culture were embedded in paraffin blocks, which were sliced at 4-μm thickness. The antigen was retrieved by using L.A.B. (Liberate Antibody Binding) solution (Polysciences), except in the case of type X collagen antigen retrieval with hyaluronidase digestion. CAS block was used for blocking except for the cultured bones, which were blocked by using 5% bovine serum albumin in PBS. Blocked sections were incubated with anti-type X collagen (1:50, LB-0092, LSL), anti-TGF-β1 (1:50, sc146, Santa Cruz Biotechnology, Inc.), anti-phospho-Smad2 (1:100, catalog no. 3103, Cell Signaling), anti-phospho-Smad3 (1:500, catalog no. 600-401-919, Rockland), anti-Smad2/3 (1:100, catalog no. 610842, BD Biosciences), anti-SnoN (1:50, H-317, sc-9142, Santa Cruz Biotechnology, Inc.), and anti-V5-FITC (1:50, R963-25, Invitrogen). Signals were detected using the REAL EnVision detecting system with DAB chromogen (Dako), anti-rabbit Alexa Fluor 488 (1:200, A11008), or anti-mouse Alexa Fluor 546 (1:200, A11060) (Invitrogen).

Real-time Quantitative PCR Assay—Cells were lysed with the TRIzol reagent (Invitrogen) to purify RNA, and 1 μg of RNA was reverse transcribed into cDNA by using the Verso cDNA Kit (Thermo Scientific). The relative amount of gene transcripts was determined by real-time PCR using the THUNDERBIRD quantitative PCR (qPCR) mix (Toyobo) on the Thermal Cycler Dice TP850 (Takara). PCRs were performed in duplicate, and the measured expression level of each gene was normalized to that of *Hprt1*. Sequence information of primers used is listed in supplemental Table 1.

Luciferase Assay—COS-7 cells were seeded in triplicate in 24-well plates and transiently transfected with firefly reporter constructs, pGL4.75hRlucCMV *Renilla* vector, constitutively active type I receptor constructs, and the SnoN vector. Dual luciferase assays were performed as described (30) using the GloMax 96 microplate luminometer (Promega).

Statistical Analysis—Data in this study are expressed as the mean ± S.D. of at least three independent experiments. A p value of <0.05, which was determined by Student's t test, was accepted as statistically significant.

RESULTS

Endogenous TGF-β Signaling Suppresses Terminal Chondrocyte Maturation in Bone—To identify physiologically active target genes of TGF-β signaling in chondrocytes, we employed

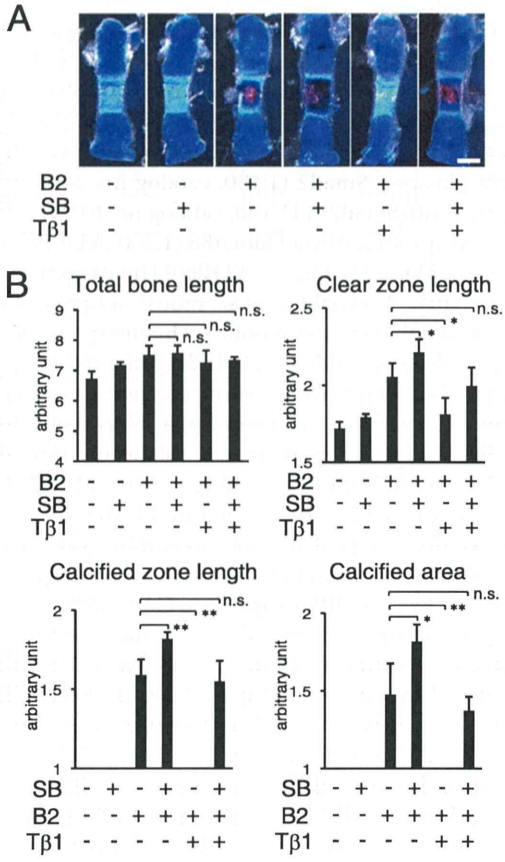

FIGURE 1. **Endogenous TGF-β signaling prevents maturation of chondrocytes in bone organ culture.** Metatarsal bones from E17.5 mouse embryo were cultured with BMP-2 (*B2*; 300 ng/ml) or TGF-β1 (*Tβ1*; 5 ng/ml) in combination with SB431542 (*SB*; 1 μM) for 4 days. *A*, cartilage matrix was stained with Alcian blue, whereas chondrocyte matrix calcified by mature hypertrophic chondrocytes was stained by alizarin red. The clear zone represented hypertrophic chondrocytes. *B*, total bone length, clear zone length, calcified zone length, and calcified area, were analyzed on images using ImageJ software ($n = 4$). *, $p < 0.05$; **, $p < 0.01$; *n.s.*, not significant. *Error bars*, S.D.

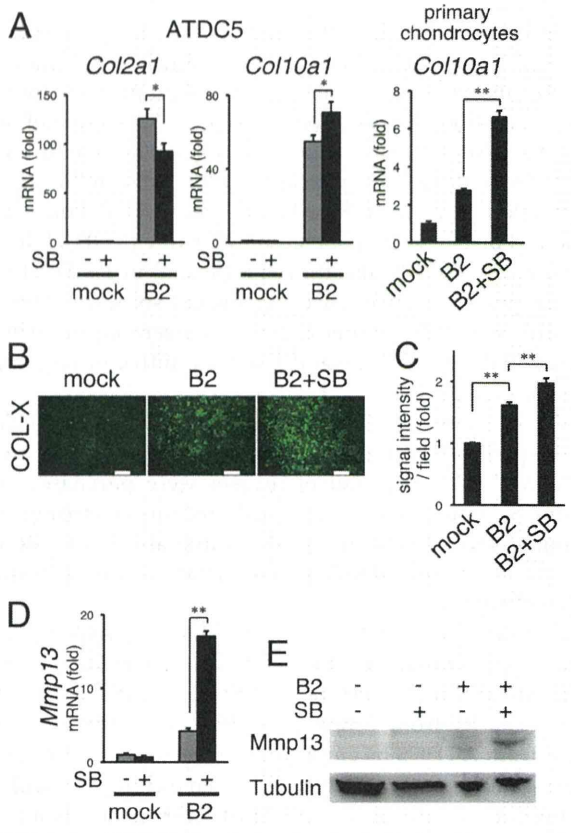

FIGURE 2. **Loss of TGF-β signaling promotes hypertrophic conversion of chondrocytes.** *A*, expression of *Col2a1* and *Col10a1* in ATDC5 chondrocytes and mouse primary chondrocytes was analyzed by qPCR. Cells were treated with or without BMP-2 (*B2*; 300 ng/ml) in combination with SB431542 (*SB*; 1 μM). ATDC5 cells were harvested at day 5, whereas primary chondrocytes were harvested at day 14. *B* and *C*, immunocytochemistry for type X collagen (*COL-X*) was performed on micromass cultures of ATDC5 cells at day 10. *Scale bars*, 200 μm. The fluorescent signal of immunocytochemistry was quantified by ImageJ software for four independent fields per group (*C*). *D*, expression of *Mmp13* mRNA was evaluated by qPCR. *E*, expression of Mmp13 protein in ATDC5 cells at day 18 was assessed by immunoblotting. Tubulin served as a loading control. *, $p < 0.05$; **, $p < 0.01$. *Error bars*, S.D.

a TGF-β type I receptor kinase inhibitor, SB431542, to block endogenous TGF-β signaling. First, we evaluated if SB431542 could accelerate chondrocyte hypertrophy and, subsequently, matrix calcification in mouse embryonic metatarsal bone organ cultures, which is a system that allows for the study of complex chondrogenic processes in a three-dimensional structure in the context of native cell-cell and cell-extracellular matrix interactions and cellular signaling (29). The cartilage matrix was stained by Alcian blue, whereas the matrix calcified by mature hypertrophic chondrocytes was stained by alizarin red; the clear zone represented uncalcified hypertrophic chondrocytes (Fig. 1*A*). Upon treatment with BMP-2, matrix calcification was induced, whereas coapplication of TGF-β1 prevented the chondrocyte maturation. Blocking of endogenous TGF-β signaling by SB431542 in BMP-treated bone significantly enhanced the length of the clear zone as well as both length and area of the calcified matrix of cartilage; this effect was diminished by exogenous TGF-β1 application (Fig. 1, *A* and *B*). The longitudinal bone growth was slightly promoted by BMP-2, whereas SB431542 or TGF-β1 showed no effect. These results confirmed the inhibitory action of endogenous TGF-β signaling in chondrocyte hypertrophy and maturation in bone rudiments.

Next, to investigate cell-autonomous actions of endogenous TGF-β signaling in BMP-induced maturation of chondrocytes, we applied SB431542 in a chondrocyte micromass culture, which is a system widely employed to study the multiple steps of cartilage differentiation (31). Upon treatment with BMP-2 in the presence of insulin/transferrin/selenium supplements, expression of *Col2a1* and *Col10a1* was induced in ATDC5 cells, as reported previously (32), whereas combined application of SB431542 mildly suppressed the level of *Col2a1* mRNA, suggesting the promotive role of TGF-β signaling in early chondrogenesis (Fig. 2*A*). In contrast, BMP-induced expression of *Col10a1* was further enhanced by SB431542 in ATDC5 cells as well as dramatically enhanced in mouse primary chondrocytes (Fig. 2*A*). Whereas treatment with BMP-2 accelerated the production of the type X collagen protein (encoded by *Col10a1*) in ATDC5 cells, SB431542 further strengthened the signal (Fig. 2*B*). The fluorescent signal of immunocytochemistry against type X collagen was significantly increased by SB431542 treat-

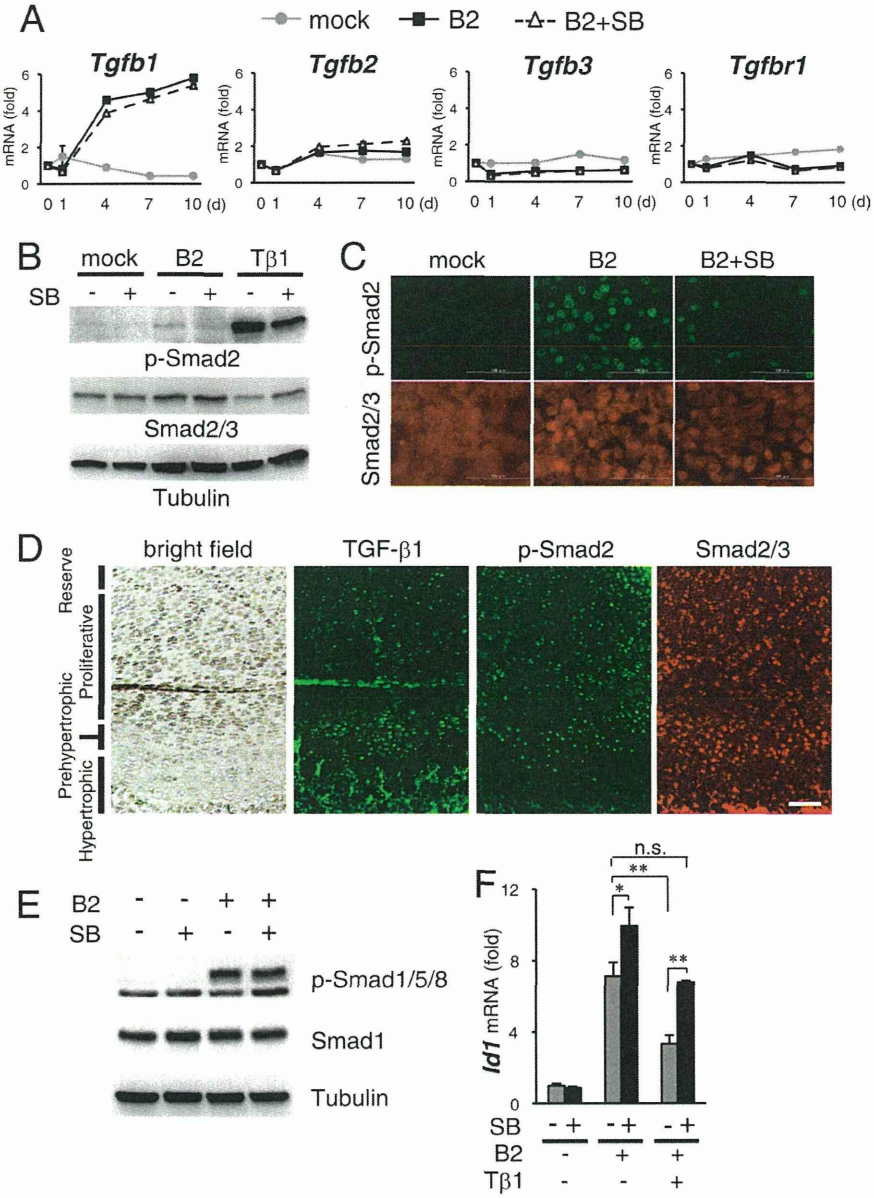

FIGURE 3. **Endogenous TGF-β signaling is activated in maturing chondrocytes to suppress the expression of *Id1*, a direct target gene of BMP-Smad pathway.** *A*, ATDC5 chondrocytes were cultured with BMP-2 (*B2*; 300 ng/ml) in combination with SB431542 (*SB*; 1 μM) for the indicated times. Expression of *Tgfb1*, *Tgfb2*, *Tgfb3*, and *Tgfbr1* were examined by qPCR. *B*, status of TGF-β signaling activity was evaluated by immunoblotting for phosphorylated Smad2 (*p-Smad2*). ATDC5 cells were stimulated with BMP-2 for 7 days or TGF-β1 (*Tβ1*; 5 ng/ml) for 1 h, with or without SB431542. Immunoblot for tubulin served as loading control. *C*, status of TGF-β signaling activity was evaluated by immunocytochemistry for phosphorylated Smad2. ATDC5 cells were stimulated with BMP-2 for 4 days with or without SB431542. *D*, expression of TGF-β1 and status of intracellular TGF-β signaling activity (*p-Smad2*) in mouse E17.5 humerus cartilage were evaluated by immunohistochemistry. *E*, status of BMP signaling activity was evaluated by immunoblotting for phosphorylated Smad1/5/8 (*p-Smad1/5/8*). ATDC5 cells were stimulated with BMP-2 for 4 days, with or without SB431542. Immunoblot for tubulin served as loading control. *F*, expression of *Id1* in ATDC5 cells at day 5 of stimulation was evaluated by qPCR. *Scale bar*, 100 μm. *, $p < 0.05$; **, $p < 0.01$; *n.s.*, not significant. *Error bars*, S.D.

ment (Fig. 2*C*). Moreover, the expression of *Mmp13*, encoding the collagenase matrix metallopeptidase 13 specifically expressed by the terminal hypertrophic chondrocytes, was dramatically up-regulated by blockade of the TGF-β signaling pathway at both mRNA and protein levels (Fig. 2, *D* and *E*). These data demonstrate the cell-autonomous inhibitory action of endogenous TGF-β signaling in the late stage of chondrocyte differentiation.

Endogenous TGF-β Signaling Is Up-regulated during Maturation of Chondrocytes—Because SB431542 affected the late stage of chondrocyte differentiation, we assessed if the expression of any of the three TGF-β ligands was increased during BMP-induced maturation of ATDC5 chondrocytes. Although the mRNA levels of *Tgfb2* and *Tgfb3* were marginally changed by application of BMP-2 or SB431542, *Tgfb1* (encoding TGF-β1) was dramatically increased from day 4 and further remained up-regulated by BMP-2 treatment, whereas it was not affected by SB431542 (Fig. 3*A*). Because TGF-β ligands transduce the signal through TGF-β type I receptor ALK5, encoded by *Tgfbr1*, we asked if expression of *Tgfbr1* was accelerated in maturing ATDC5 cells. However, the expression level of *Tgfbr1* was unchanged by BMP-2 application (Fig. 3*A*). Therefore, we

evaluated if increased *Tgfb1* expression reflected intracellular signal transduction (Fig. 3*B*). As a positive control, exogenously applied TGF-β1 potently induced the C-terminal phosphorylation of Smad2, which was weakened by SB431542. Importantly, in BMP-2-treated ATDC5 chondrocytes, Smad2 was phosphorylated at a comparatively weak but detectable level, which was suppressed by SB431542 (Fig. 3*B*). In addition, an immunocytochemistry for phosphorylated Smad2 in ATDC5 cells showed that endogenous TGF-β signaling was activated in BMP-2-treated chondrocytes, which was blocked by SB431542 (Fig. 3*C*). These data indicated that the activation of Smad2 by BMP-2 was achieved through the TGF-β type I receptor, probably by the up-regulated production of TGF-β1 in ATDC5 cells. In developing humerus growth plate of E17.5 mouse embryo, moderate expression of TGF-β1 was detected in proliferative chondrocytes, suggesting its role in promoting early chondrogenesis (Fig. 3*D*). Importantly, the expression of TGF-β1 was further accentuated in the prehypertrophic zone and the matrix around the hypertrophic chondrocytes (Fig. 3*D*). Similarly, Smad2 was phosphorylated in some of the proliferative chondrocytes, whereas phospho-Smad2 was detected in most of the prehypertrophic chondrocytes (Fig. 3*D*). Interestingly, Smad2 was not phosphorylated in hypertrophic chondrocytes. These results from immunohistochemistry suggested that expression of TGF-β1 was elevated to up-regulate TGF-β signaling in prehypertrophic chondrocytes, whereas the signaling was inhibited with in hypertrophic chondrocytes, in the endochondral ossification process.

Because Smad3 signaling had been suggested to suppress BMP pathway in maturing chondrocytes (26), we examined immunoblotting for the phosphorylated Smad1/5/8 to investigate the role of endogenous TGF-β signaling against the BMP-Smad signaling system in chondrocytes. BMP-2 induced potent C-terminal phosphorylation of Smad1/5/8 in ATDC5 cells, even at day 4 of induction, whereas combined treatment with SB431542 showed no effect (Fig. 3*E*). However, interestingly, the expression of *Id1*, a specific direct target of the canonical BMP-Smad pathway (33), was significantly elevated by SB431542 treatment, whereas it was suppressed by exogenously applied TGF-β1 (Fig. 3*F*). These data suggest that BMP-induced activation of endogenous TGF-β signaling inhibited BMP signaling downstream of R-Smad activation as a negative feedback mechanism. These data also confirmed that SB431542 is an appropriate tool to screen for putative molecular mediator(s) downstream of endogenous TGF-β signaling to inhibit BMP signaling in chondrocytes.

SnoN Is Induced by Endogenous TGF-β Signaling in Maturing Chondrocytes—The BMP signaling system is negatively regulated at multiple steps (*e.g.* by extracellular antagonists (*e.g.* Noggin, Chordin, Dan, and Cerberus), inhibitory Smads (I-Smads; Smad6 and Smad7), E3 ubiquitin ligases (*e.g.* Smurf1 and Smurf2), and the Ski/SnoN family of transcriptional corepressors) (34, 35). We asked if any of these BMP signaling inhibitors were induced downstream of endogenous TGF-β signaling in maturing chondrocytes. In micromass cultures of ATDC5 chondrocytes, treatment with TGF-β1, as positive control, significantly elevated only the expression of *Smad7* and *SnoN*, both of which are the direct target genes of the TGF-β-Smad pathway (supplemental Fig. 1). In BMP-2-induced maturing cells, *Smad6*, *Smad7*, and *SnoN* were up-regulated, whereas combined treatment with SB431542 completely inhibited only the elevation of *SnoN* (supplemental Fig. 1). In mouse primary chondrocytes at day 14 of BMP treatment, SnoN was also significantly elevated; this effect was not observed by combined application with SB431542 (Fig. 4*A*). These data indicate that, among the examined BMP inhibitors, SnoN was exclusively induced by the enhanced endogenous TGF-β signaling in maturing chondrocytes. During the maturation phase of ATDC5 chondrocytes, the level of *SnoN* mRNA was increased from days 4 to 10 of BMP application and mildly decreased thereafter, whereas this effect was completely prevented by SB431542 (Fig. 4*B*). Because SnoN is an unstable protein, which has a half-life of 30 min in the presence of TGF-β signaling (36, 37), we asked if the protein level of SnoN reflects the pattern of its mRNA expression and performed an immunoblot for SnoN protein (Fig. 4*C*). As control to identify specific bands for endogenous SnoN protein, we performed a knockdown assay against *SnoN* in monolayer cultures of ATDC5 cells (Fig. 4*C*, *lanes 5–7*). At day 3, the signals of two major bands of around 80 kDa were increased in BMP-2-treated cells, both of which were efficiently abolished by siSnoN, indicating that these bands represented the two isoforms, SnoN and SnoN2 (38). In micromass cultures of ATDC5 chondrocytes at day 7 of BMP-2 application, SnoN protein expression was also induced and further weakened by SB431542 (Fig. 4*C*, *lanes 1–4*), indicating that the expression of the SnoN protein was indeed induced by endogenous TGF-β signaling in maturing chondrocytes. We also confirmed the induction of SnoN protein by immunocytochemistry. Treatment with TGF-β1 for 16 h potently increased the signal of SnoN protein, which was only faintly detected in cells transfected with SnoN siRNA (Fig. 4*D*). At day 4 of BMP-2 stimulation, the level of SnoN protein was up-regulated, which was weakened by siSnoN, in maturing ATDC5 chondrocytes of monolayer cultures (Fig. 4*E*). The knockdown efficiency of SnoN in BMP-2-treated cells was relatively weak, probably because 5 days had passed since the transfection of siRNA. Next, to confirm that the inhibitory effect of SB431542 against the expression level of *SnoN* was exclusive for the late maturation phase, we stimulated ATDC5 cells with BMP-2 in combination with SB431542 and harvested the cells at the early time points within 36 h of induction (Fig. 4*F*). To our surprise, *SnoN* was rapidly induced by BMP-2 after 1 h and was decreased to reach the basal level thereafter, an expression pattern that was similar to that of *Id1* (Fig. 4*F*). However, this transient induction of *SnoN* by BMP-2 was not affected by SB431542, suggesting that endogenous TGF-β signaling was not responsible for this up-regulation of *SnoN*.

To investigate the possibility that SnoN plays a role in chondrogenesis *in vivo*, its expression in cartilage tissue was examined. We extracted RNA from various tissues of 3-month-old adult mice to prepare tissue panels of cDNA to analyze the tissue distribution. Consistent with the report that heterozygous *SnoN* knock-out mice developed T lymphomas in the spleen, which indicates an important role of SnoN in the spleen (39), we detected the highest level of *SnoN* expression in the spleen (Fig. 4*G*). Interestingly, the comparatively highest level

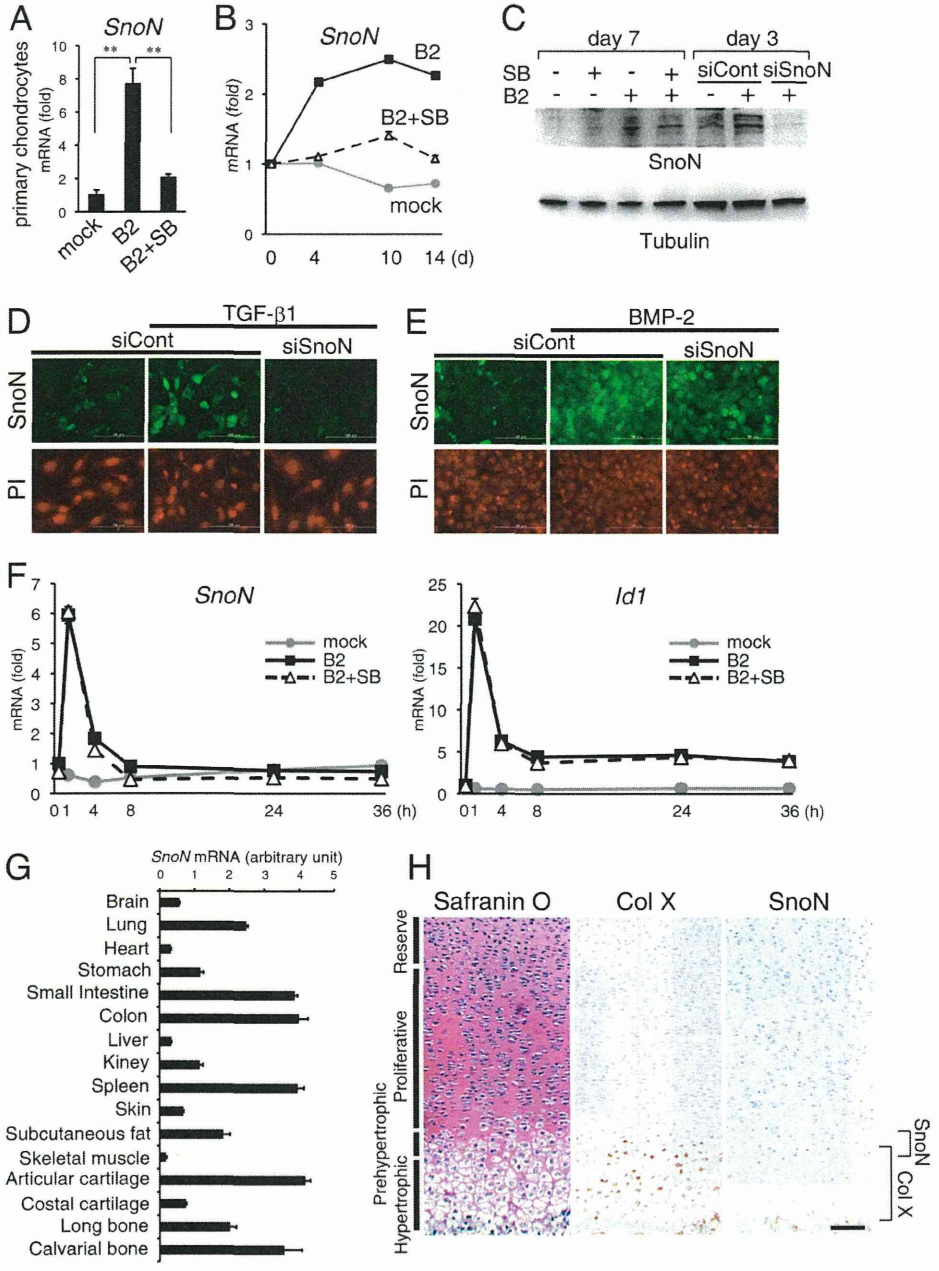

FIGURE 4. **SnoN is induced in maturing chondrocytes by endogenous TGF-β signaling *in vitro*, whereas it is highly expressed in cartilage tissue in mice.** *A*, expression of *SnoN* in primary chondrocytes at day 14 of stimulation was evaluated by real-time RT-PCR. Cells were stimulated with BMP-2 (*B2*; 300 ng/ml) with or without SB431542 (*SB*; 1 μM). *B*, ATDC5 chondrocytes were cultured with BMP-2 with or without SB431542 for the indicated times, after which the samples were subjected to qPCR analysis for *SnoN*. *C*, expression of SnoN protein in ATDC5 cells was assessed by immunoblotting. Differentiation of ATDC5 cells was induced by incubation with BMP-2 for 7 days (*lanes 1–4*). As a control, cells were transfected with siSnoN for 16 h and further cultured in the presence of BMP-2 for 3 days (*lanes 5–7*). Tubulin served as a loading control. *D* and *E*, immunocytochemistry for SnoN was performed on a monolayer culture of ATDC5 cells. Cells were transfected with siRNA for 16 h and further incubated with or without TGF-β1 (5 ng/ml) for 16 h (*D*) or with or without BMP-2 for 4 days (*E*). MG132 (10 μM) was applied 16 h prior to cell fixation. Nuclei were visualized with propidium iodide (*PI*). *Scale bars*, 100 μm. *F*, ATDC5 chondrocytes were stimulated with BMP-2 in combination with SB431542 for the indicated time points. cDNA samples were subjected to qPCR analysis for *SnoN* and *Id1*. *G*, tissue cDNA panel of 3-month-old mice was subjected to real-time PCR for *SnoN*. *H*, protein expression of type X collagen (*Col X*) and SnoN in E17.5 humerus cartilage was determined by immunohistochemistry. Zones of positive signal were indicated. Proteoglycans in cartilage matrix were stained by Safranin O. *Scale bar*, 100 μm. **, $p < 0.01$. *Error bars*, S.D.

of *SnoN* expression was found in articular cartilage (Fig. 4*G*). Immunohistochemistry for the growth plate of developing bone of mouse embryos at E17.5, in which endochondral ossification was in progress, detected the signal of type X collagen protein from the lower half of prehypertrophic chondrocytes to the entire area of hypertrophic chondrocytes (Fig. 4*H*). Importantly, although SnoN protein was detected weakly in proliferating chondrocytes, its potent signal was present in prehypertrophic chondrocytes, whereas it was weakened in hypertrophic chondrocytes (Fig. 4*H*). These data suggest that SnoN is highly expressed in premature chondrocytes before hypertrophic conversion, *in vitro* and *in vivo*.

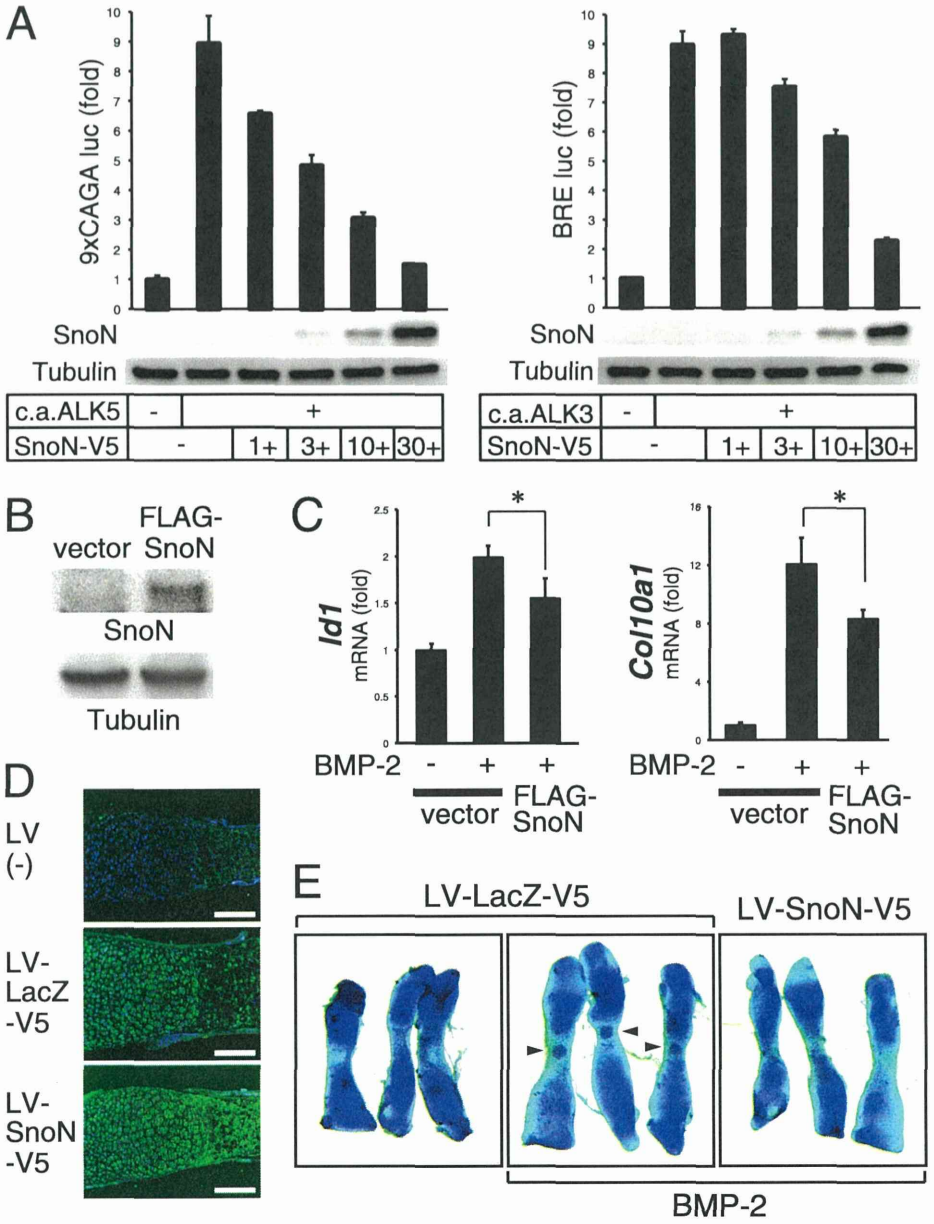

FIGURE 5. **SnoN suppresses BMP signaling and subsequent chondrocyte maturation.** *A*, SnoN expression vector was transfected with plasmids of constitutively active type I receptors and a luciferase reporter of 9xCAGA luc (for TGF-β signaling) or BRE luc (for BMP signaling) into COS-7 cells. Expression of transfected SnoN was confirmed by anti-SnoN immunoblot. Tubulin served as loading control. *B*, FLAG-tagged SnoN expression vector was stably transfected into ATDC5 chondrocytes, and its expression was confirmed by anti-SnoN immunoblotting. *C*, SnoN suppressed expression of *Id1* as well as *Col10a1* at day 7 of BMP-2 (300 ng/ml) treatment in a stable transfectant of ATDC5 chondrocytes. *D* and *E*, metatarsal bones of E17.5 mouse embryo were infected with indicated lentivirus (*LV*) for 16 h. Immunostaining using FITC-linked anti-V5 antibody on bone coronal sections was performed at day 2 of culture to evaluate the efficiency of lentiviral infection. Nuclei were stained with Hoechst dye. Merged images are presented. LV-LacZ-V5 served as a lentiviral infection control (*D*). *Scale bars*, 200 μm. Alcian blue/alizarin red staining was performed at day 2 of BMP-2 treatment (*E*). The *arrowheads* indicate the calcified cartilage matrix in bone rudiments of triplicate culture. *, $p < 0.05$. *Error bars*, S.D.

SnoN Suppresses the BMP-Smad Signaling Pathway to Inhibit Hypertrophic Maturation of Chondrocytes—SnoN interacts with Smad2, Smad3, and Smad4 in the cytoplasm to prevent their nuclear translocation (40, 41). In the nucleus, it represses their transcriptional activity by disrupting the active trimeric Smad complex and recruiting transcriptional corepressors (36), thereby negatively regulating TGF-β signaling. It is not known whether SnoN suppresses canonical BMP-Smad signaling in the same manner as the related family molecule c-Ski (42); however, SnoN may inhibit the pathway because of its ability to bind Smad4, although it cannot bind Smad1/5/8 (43). To test this hypothesis, SnoN was investigated using a BRE luciferase reporter specifically responding to the BMP-Smad pathway (33) in COS-7 cells. As a positive control for the SnoN function, SnoN was applied to the 9xCAGA TGF-β signal reporter (44), activated by constitutively active TGF-β type I receptor ALK5, to show a dose-dependent potent inhibition (Fig. 5*A*, *left*). Interestingly, SnoN did suppress the activity of

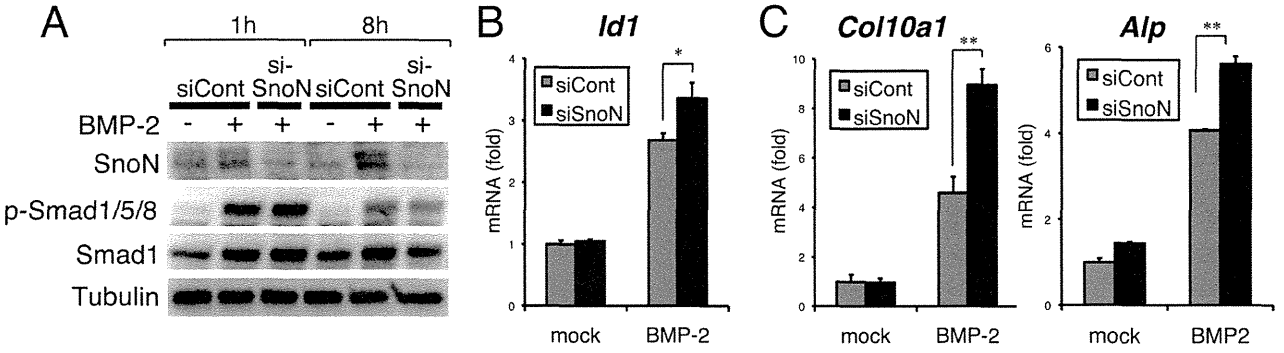

FIGURE 6. **Loss of SnoN in ATDC5 chondrocytes mimics the effect of SB431542, which accelerates the expression of *Id1* and hypertrophic marker genes.** *A*, ATDC5 cells were stimulated by BMP-2 (300 ng/ml) 16 h after transfection with siRNA. Cells harvested at the indicated time points were subjected to immunoblotting. *B* and *C*, ATDC5 chondrocytes were transfected with siRNA for 16 h, followed by induction of differentiation with BMP-2 for 3 days. Expression of *Id1*, *Col10a1*, and *Alp* was analyzed by real-time RT-PCR. *, $p < 0.05$; **, $p < 0.01$. *Error bars*, S.D.

the BRE reporter induced by the constitutively active type I BMP receptor ALK3 (encoded by *Bmpr1a*) (Fig. 5*A*, *right*) in a dose-dependent manner, although more than 3 times the amount of SnoN plasmid DNA was required for the inhibition compared with the reporter assay using 9xCAGA. Next, we stably transfected a FLAG-tagged SnoN expression vector into ATDC5 cells and confirmed the transgene expression by anti-SnoN immunoblotting (Fig. 5*B*). In ATDC5 chondrocytes, gain of SnoN suppressed the elevated expression of *Id1* at day 7 of BMP-2 induction (Fig. 5*C*, *left*). The increased expression of the hypertrophic marker *Col10a1* was also down-regulated by SnoN in BMP-treated ATDC5 cells (Fig. 5*C*, *right*). Thus, forced expression of SnoN in ATDC5 chondrocytes inhibited BMP signaling and, subsequently, chondrocyte maturation. To investigate the role of SnoN in cartilage maturation, we infected lentivirus carrying V5-tagged SnoN expression cassette into E17.5 metatarsal bone rudiments. We confirmed the infection efficiency of the lentivirus by performing immunohistochemistry on the coronal sections of the bones, using anti-V5-FITC antibody to detect the transgene product (Fig. 5*D*). In lentivirus-infected bones, we found the certain expression of V5-tagged transgenes in the cells of perichondrium and the chondrocytes in zones of reserve, proliferative, and prehypertrophic but not hypertrophic chondrocytes. Treatment of BMP-2 induced calcification of the hypertrophic zone of bone rudiments (Fig. 5*E*, *arrowheads*), whereas overexpression of SnoN by lentivirus completely prevented the cartilage mineralization (Fig. 5*E*). These data demonstrate that gain of SnoN inhibits the maturation of the hypertrophic chondrocytes.

Next, we investigated the physiological role of endogenous SnoN in ATDC5 chondrocytes by performing an siRNA-mediated knockdown assay. We confirmed that SnoN protein expression was induced upon BMP-2 induction, even at the early time points, and that the two bands (representing SnoN and SnoN2) could be efficiently eliminated by siSnoN (Fig. 6*A*). BMP-2 induced a potent phosphorylation of Smad1/5/8, whereas siSnoN showed no effect on the phosphorylation level, even after the phosphorylation declined at 8 h (Fig. 6*A*). However, knockdown of SnoN mildly, but significantly, enhanced the BMP-2-induced increase of the *Id1* gene at day 4 in ATDC5 cells (Fig. 6*B*). siSnoN further significantly enhanced the BMP-induced up-regulation of *Col10a1* as well as alkaline phosphatase (*Alp*), another marker of matured hypertrophic chondrocytes (Fig. 6*C*). These data for the SB431542-mimicking effects of siSnoN (Figs. 2 and 3) indicated that SnoN mediated a major part of the roles of endogenous TGF-β signaling in chondrocytes to physiologically suppress BMP signaling and subsequent chondrocyte hypertrophic maturation without affecting the activating step of Smad1/5/8.

TGF-β Signaling and Expression of SnoN Are Accentuated in "Prehypertrophic" Chondrocytes Adjacent to Pathologically Hypertrophic Chondrocyte in Moderately Affected OA Cartilage—Given the role of SnoN in the prevention of hypertrophic conversion of chondrocytes, SnoN protein may be present before pathologic chondrocytes gained hypertrophic phenotype in OA cartilages (8, 9). We performed immunohistochemistry assays for SnoN in human OA cartilages of various severities. In normal adult human femoral head cartilage, expression of type X collagen was entirely absent, whereas SnoN protein was weakly detected in the superficial zone (Fig. 7*A*). In moderate OA cartilage, in which the severity was graded as 6 according to the modified Mankin score (45, 46), type X collagen-positive pathologically hypertrophic chondrocytes were located in the upper layer of degenerated cartilage, which was poorly stained by Safranin O. Strikingly, we detected potent signals for SnoN protein in chondrocytes in which the cell body was mildly enlarged, resembling "prehypertrophic" chondrocytes in the developing bone. These SnoN-positive cells formed colonies located in close proximity of the colonies of hypertrophic chondrocytes (Fig. 7*A*). In severe OA cartilage of a grading score of 10, the cartilage surface of which was entirely destroyed, a few colonies of pathologically hypertrophic chondrocytes expressing type X collagen were present; however, we could no longer detect SnoN-positive cells (Fig. 7*A*). These data are consistent with our hypothesis that SnoN prevents the progression of hypertrophic conversion of articular chondrocytes. Finally, we asked if this enhanced expression of SnoN protein was associated with TGF-β signaling in human OA cartilage, similarly as observed in the growth plate of mouse embryo (Figs. 3*D* and 4*H*). In moderate OA cartilage, an immunofluorescence assay revealed the abundant accumulation of TGF-β1 protein around the "prehypertrophic" chondrocytes (Fig. 7*B*). Moreover, phosphorylated active Smad3 was detected in these pathologic chondrocytes. Again, SnoN protein was also expressed in chon-

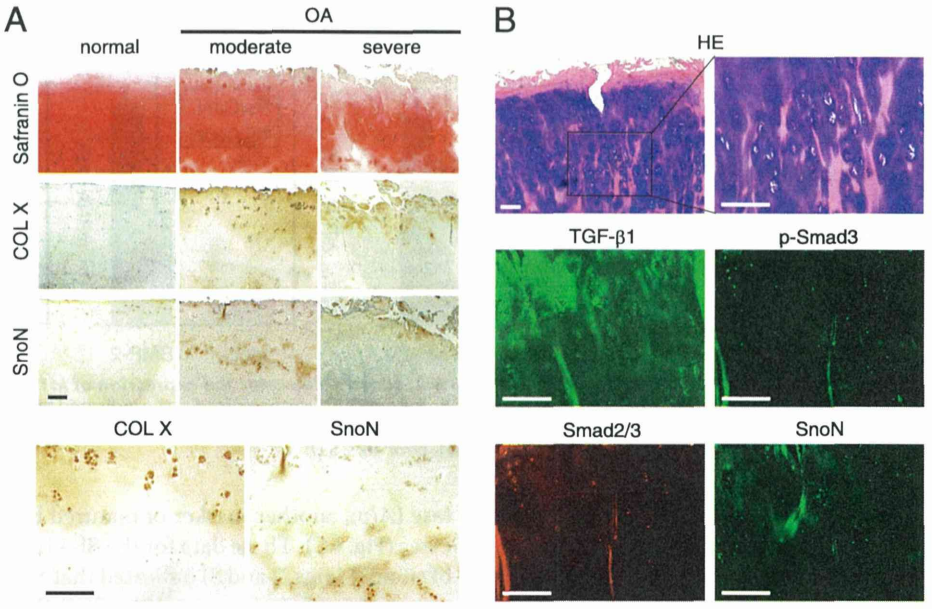

FIGURE 7. **TGF-β signaling and expression of SnoN are up-regulated in mildly hypertrophic chondrocytes located adjacent to colonies of pathologically hypertrophic chondrocytes in human OA cartilage.** *A*, human OA cartilage samples were subjected to immunohistochemistry for type X collagen (*COL X*) and SnoN. The severity of OA was graded according to the modified Mankin score on the basis of the histology of cartilage specimens stained with Safranin O. *Bottom panel*, magnified images of a moderate OA sample in the *top panel*. *B*, the human OA cartilage specimen of moderate severity was subjected to hematoxylin and eosin (*HE*) staining and immunohistochemistry for TGF-β1, phosphorylated Smad3 (*p-Smad3*), total Smad2/3, and SnoN. *Scale bars*, 200 μm.

drocytes in this region. These data demonstrated an association of TGF-β signaling and expression of SnoN in the degenerating cartilage.

DISCUSSION

Endogenous TGF-β Signaling Is Activated in Maturing Chondrocytes to Induce SnoN—Although the importance of TGF-β signaling in preventing hypertrophic conversion of chondrocytes has been demonstrated (23, 24, 47), the mode of TGF-β signaling during chondrocyte maturation and its direct target gene(s) responsible for inhibiting the differentiation remain largely unknown. While exogenously applied TGF-β has been reported to have a positive role in early chondrogenesis *in vitro*, SB431542 showed no effect on bone growth, whereas it dramatically enhanced the matrix calcification by the mature hypertrophic chondrocytes in a bone organ culture system (Fig. 1). This result suggested that endogenous TGF-β signaling was more active in the late stage of maturing chondrocytes than in the early stage of chondrocyte differentiation. Indeed, expression of *Tgfb1* was up-regulated in the late phase of differentiation of ATDC5 chondrocytes (Fig. 3*A*), coupled with an increase in phosphorylation of Smad2, which was inhibited by SB431542 (Fig. 3, *B* and *C*). This was completely linked to the expression pattern of SnoN (Fig. 4, *A*–*C*). SnoN expression was probably directly induced by endogenous TGF-β signaling because *SnoN* had been shown to be directly induced by TGF-β-activated Smad2 through its binding to the Smad-binding element in the promoter of the *SnoN* gene (48). Interestingly, in Smad3-deficient chondrocytes, the expression of TGF-β1, TGF-β type I receptor ALK5 (*Tgfbr1*), and SnoN was suppressed, whereas the expression of Smad1, Smad5, Smad6, BMP-2, and BMP-6 was elevated (26), suggesting SnoN to be one of the downstream targets of TGF-β signaling in chondrocytes. For the first time, we demonstrated the rapid and transient induction of *SnoN* by exogenously applied BMP ligand, whereas it was not suppressed by SB431542 (Fig. 4*F*). The *SnoN* expression pattern in the early phase, which resembled that of *Id1* (Fig. 4*F*), led us to hypothesize that the BMP-Smad pathway, in addition to TGF-β-Smad signaling, can directly induce *SnoN* in a context-dependent manner. Indeed, the sequences of GGCACC or GGCGCG, both of which contain a 1-base mismatch with the BMP-Smad-responsive motif GGCGCC (33), can be found adjacent to three TGF-β-responsive CAGA Smad-binding elements in the *SnoN* promoter (48). Further experiments are required to resolve this hypothesis and to evaluate the roles of BMP-Smad-induced SnoN.

SnoN Interferes with BMP Signaling to Suppress Hypertrophic Differentiation of Chondrocytes—The *Sno* gene (whose name derived from "*Ski*-related novel gene") was initially discovered on the basis of its close homology to v-Ski and c-Ski. Ski proteins can suppress TGF-β signaling, as well as BMP signaling, by binding to R-Smads and Smad4. Interestingly, although c-Ski can interact weakly with Smad1/5, the strong interaction with Smad4 is indispensable for suppression of BMP signaling by c-Ski (42). Although SnoN interacts with Smad4, the role of SnoN in the context of BMP signaling has not been well investigated. We showed here that SnoN suppressed BMP signaling in a comparative but slightly weaker manner compared with TGF-β signaling (Fig. 5*A*). This weaker suppression of BMP signaling is probably due to the difference in the accessibility to Smads (*i.e.* SnoN could bind to Smad2/3 and Smad4 but not to Smad1/5, unlike c-Ski) (43). Loss of SnoN mildly enhanced the expression of *Id1*, whereas it did not affect the phosphorylation level of Smad1/5/8 (Fig. 6, *A* and *B*), supporting the notion that the functional molecular target of SnoN was not the phosphor-

ylation step of Smad1/5/8 but rather Smad4. Because siSnoN and SB431542 showed an essentially similar effect with regard to phospho-Smad1/5/8 and *Id1* expression (compare Fig. 3, *E* and *F*, and Fig. 6, *A* and *B*), SnoN seems to be one of the major mediators of TGF-β signaling to inhibit BMP signaling in chondrocytes. This is interesting because we previously reported a similar negative feedback mechanism regulated by signal crosstalk between TGF-β and BMP signaling in osteoblast differentiation, in which I-Smads were induced by endogenous TGF-β signaling to inhibit BMP signaling in the maturation phase (49). However, the expression of I-Smads was not dramatically affected by SB431542 in ATDC5 chondrocytes (supplemental Fig. 1), suggesting context-dependent mechanisms in the selection of TGF-β target genes in these mesenchymal cells. The effect of forced expression, or knockdown, of SnoN showed more dramatic changes in the *Col10a1* expression than in that of *Id1* (Figs. 5*C* and 6*C*). The persistently mild suppression of BMP signaling by SnoN during the maturing phase may account for the major inhibition of hypertrophic maturation of chondrocytes.

Expression of SnoN Is Associated with the Enhanced TGF-β Signaling in Prehypertrophic Chondrocytes in Mouse Developing Bone and Human OA Cartilage—Maintenance of the articular cartilage depends on the function of articular chondrocytes, which produce cartilage matrix and are constrained from undergoing the maturation program seen in growth plate chondrocytes of developing bone. Genetic association of single nucleotide polymorphisms (SNPs) in the *SMAD3* or *ASPN* gene (encoding asporin) with human OA has been reported (50, 51). Asporin was shown to bind TGF-β ligands on the cell surface to block their signal transduction (52). In articular cartilage of old mice, decreased expression of TGF-β ligands and receptors, coupled with strongly dropped phosphorylation of Smad2, was observed (53). Moreover, as mentioned in the Introduction, mouse models of loss of TGF-β signaling showed an OA phenotype with accelerated hypertrophic conversion of chondrocytes. These lines of evidence clearly demonstrate the importance of TGF-β signaling in preventing OA change of articular chondrocytes. To date, the mechanism by which TGF-β signaling regulates this process is largely unknown. One candidate for targeting TGF-β signaling is Smurf2, a protein whose expression was up-regulated in human OA cartilage, whereas forced expression of Smurf2 in chondrocytes developed OA change in joints of the transgenic mice (25). Because Smurf2 is a TGF-β-inducible molecule to inhibit TGF-β signaling, it may mediate the effect of TGF-β signaling in chondrocyte hypertrophy. However, in *Smad3*-deficient chondrocytes, which showed enhanced BMP signaling and accelerated maturation, expression of *Smurf2* was not affected (26). Similarly, in our ATDC5 micromass culture system, *Smurf2* was not elevated in maturing ATDC5 chondrocytes stimulated by BMP-2 (supplemental Fig. 1). In contrast, we detected an increase of SnoN expression, not only in both maturing ATDC5 cells and primary chondrocytes *in vitro* but also in prehypertrophic chondrocytes in mouse developing bone and in human OA cartilage (Figs. 4 and 7). Although we demonstrated the inhibitory role of SnoN in chondrocyte hypertrophy *in vitro* (Figs. 5 and 6), hypertrophy of chondrocytes was present in both developing normal mouse cartilage and degenerating human OA cartilage, despite the accentuated expression of SnoN in contiguous prehypertrophic chondrocytes (Figs. 4*H* and 7). In mouse E17.5 bone, phosphorylation of Smad2 and expression of SnoN were diminished in hypertrophic chondrocytes despite the abundant accumulation of TGF-β1 protein in the extracellular matrix (Figs. 3*D* and 4*H*), suggesting a disorder of the signal transduction by unknown mechanisms to be resolved. Similarly, in human OA cartilage, expression of SnoN was weakened in colonies of COL X-positive hypertrophic cells (Fig. 7*A*). Taken together, it is likely that the hypertrophic conversion was induced after the decline of SnoN expression in these chondrocytes. In this regard, further investigation is required to understand why the transduction of TGF-β signaling and subsequent expression of SnoN are diminished in hypertrophic chondrocytes. Although our results do not establish an etiologic role for SnoN in the progression of OA, they at least establish a strong association that explains a possible causal relationship between SnoN regulation and hypertrophic conversion of chondrocytes in OA cartilage. Loss of SnoN in mice *in vivo* should reveal its putative roles in cartilage hypertrophy or endochondral ossification; however, SnoN knock-out mice showed embryonic lethality at E3.5 (39). Therefore, a conditional knock-out mouse line of chondrocyte-specific ablation of the *SnoN* gene would be suitable to address these questions. In conclusion, our data revealed a novel role of SnoN in regulating BMP signaling and subsequent chondrocyte maturation as a downstream mediator of TGF-β signaling. SnoN may be targeted in chondrocytes to inhibit its function in order to accelerate endochondral ossification or to enhance its activity in the case of treating OA or cartilage regeneration for repair.

Acknowledgment—We gratefully acknowledge the technical assistance of Hui Gao.

REFERENCES

1. Akiyama, H., Chaboissier, M. C., Martin, J. F., Schedl, A., and de Crombrugghe, B. (2002) The transcription factor Sox9 has essential roles in successive steps of the chondrocyte differentiation pathway and is required for expression of Sox5 and Sox6. *Genes Dev.* **16,** 2813–2828
2. Provot, S., and Schipani, E. (2005) Molecular mechanisms of endochondral bone development. *Biochem. Biophys. Res. Commun.* **328,** 658–665
3. Enomoto, H., Enomoto-Iwamoto, M., Iwamoto, M., Nomura, S., Himeno, M., Kitamura, Y., Kishimoto, T., and Komori, T. (2000) Cbfa1 is a positive regulatory factor in chondrocyte maturation. *J. Biol. Chem.* **275,** 8695–8702
4. Zheng, Q., Zhou, G., Morello, R., Chen, Y., Garcia-Rojas, X., and Lee, B. (2003) Type X collagen gene regulation by Runx2 contributes directly to its hypertrophic chondrocyte-specific expression *in vivo*. *J. Cell Biol.* **162,** 833–842
5. Ueta, C., Iwamoto, M., Kanatani, N., Yoshida, C., Liu, Y., Enomoto-Iwamoto, M., Ohmori, T., Enomoto, H., Nakata, K., Takada, K., Kurisu, K., and Komori, T. (2001) Skeletal malformations caused by overexpression of Cbfa1 or its dominant negative form in chondrocytes. *J. Cell Biol.* **153,** 87–100
6. Takeda, S., Bonnamy, J. P., Owen, M. J., Ducy, P., and Karsenty, G. (2001) Continuous expression of Cbfa1 in nonhypertrophic chondrocytes uncovers its ability to induce hypertrophic chondrocyte differentiation and partially rescues Cbfa1-deficient mice. *Genes Dev.* **15,** 467–481
7. Scotti, C., Tonnarelli, B., Papadimitropoulos, A., Scherberich, A., Schaeren, S., Schauerte, A., Lopez-Rios, J., Zeller, R., Barbero, A., and Martin, I.

(2010) Recapitulation of endochondral bone formation using human adult mesenchymal stem cells as a paradigm for developmental engineering. *Proc. Natl. Acad. Sci. U.S.A.* **107,** 7251–7256
8. Pullig, O., Weseloh, G., Ronneberger, D., Käkönen, S., and Swoboda, B. (2000) Chondrocyte differentiation in human osteoarthritis. Expression of osteocalcin in normal and osteoarthritic cartilage and bone. *Calcif. Tissue Int.* **67,** 230–240
9. Sandell, L. J., and Aigner, T. (2001) Articular cartilage and changes in arthritis. An introduction. Cell biology of osteoarthritis. *Arthritis Res.* **3,** 107–113
10. Dreier, R. (2010) Hypertrophic differentiation of chondrocytes in osteoarthritis. The developmental aspect of degenerative joint disorders. *Arthritis Res. Ther.* **12,** 216
11. Nelea, V., Luo, L., Demers, C. N., Antoniou, J., Petit, A., Lerouge, S., R Wertheimer, M., and Mwale, F. (2005) Selective inhibition of type X collagen expression in human mesenchymal stem cell differentiation on polymer substrates surface-modified by glow discharge plasma. *J. Biomed. Mater. Res. A* **75,** 216–223
12. Sekiya, I., Vuoristo, J. T., Larson, B. L., and Prockop, D. J. (2002) *In vitro* cartilage formation by human adult stem cells from bone marrow stroma defines the sequence of cellular and molecular events during chondrogenesis. *Proc. Natl. Acad. Sci. U.S.A.* **99,** 4397–4402
13. Miyazono, K., Kamiya, Y., and Morikawa, M. (2010) Bone morphogenetic protein receptors and signal transduction. *J. Biochem.* **147,** 35–51
14. Tsumaki, N., Nakase, T., Miyaji, T., Kakiuchi, M., Kimura, T., Ochi, T., and Yoshikawa, H. (2002) Bone morphogenetic protein signals are required for cartilage formation and differently regulate joint development during skeletogenesis. *J. Bone Miner. Res.* **17,** 898–906
15. Yoon, B. S., Ovchinnikov, D. A., Yoshii, I., Mishina, Y., Behringer, R. R., and Lyons, K. M. (2005) Bmpr1a and Bmpr1b have overlapping functions and are essential for chondrogenesis *in vivo*. *Proc. Natl. Acad. Sci. U.S.A.* **102,** 5062–5067
16. Retting, K. N., Song, B., Yoon, B. S., and Lyons, K. M. (2009) BMP canonical Smad signaling through Smad1 and Smad5 is required for endochondral bone formation. *Development* **136,** 1093–1104
17. Furumatsu, T., Tsuda, M., Taniguchi, N., Tajima, Y., and Asahara, H. (2005) Smad3 induces chondrogenesis through the activation of SOX9 via CREB-binding protein/p300 recruitment. *J. Biol. Chem.* **280,** 8343–8350
18. Volk, S. W., Luvalle, P., Leask, T., and Leboy, P. S. (1998) A BMP-responsive transcriptional region in the chicken type X collagen gene. *J. Bone Miner. Res.* **13,** 1521–1529
19. Leboy, P., Grasso-Knight, G., D'Angelo, M., Volk, S. W., Lian, J. V., Drissi, H., Stein, G. S., and Adams, S. L. (2001) Smad-Runx interactions during chondrocyte maturation. *J. Bone Joint Surg. Am.* **83-A,** Suppl. 1, S15–S22
20. Kempf, H., Ionescu, A., Udager, A. M., and Lassar, A. B. (2007) Prochondrogenic signals induce a competence for Runx2 to activate hypertrophic chondrocyte gene expression. *Dev. Dyn.* **236,** 1954–1962
21. Kobayashi, T., Lyons, K. M., McMahon, A. P., and Kronenberg, H. M. (2005) BMP signaling stimulates cellular differentiation at multiple steps during cartilage development. *Proc. Natl. Acad. Sci. U.S.A.* **102,** 18023–18027
22. van Beuningen, H. M., Glansbeek, H. L., van der Kraan, P. M., and van den Berg, W. B. (1998) Differential effects of local application of BMP-2 or TGF-β1 on both articular cartilage composition and osteophyte formation. *Osteoarthr. Cartil.* **6,** 306–317
23. Yang, X., Chen, L., Xu, X., Li, C., Huang, C., and Deng, C. X. (2001) TGF-β/Smad3 signals repress chondrocyte hypertrophic differentiation and are required for maintaining articular cartilage. *J. Cell Biol.* **153,** 35–46
24. Serra, R., Johnson, M., Filvaroff, E. H., LaBorde, J., Sheehan, D. M., Derynck, R., and Moses, H. L. (1997) Expression of a truncated, kinase-defective TGF-β type II receptor in mouse skeletal tissue promotes terminal chondrocyte differentiation and osteoarthritis. *J. Cell Biol.* **139,** 541–552
25. Wu, Q., Kim, K. O., Sampson, E. R., Chen, D., Awad, H., O'Brien, T., Puzas, J. E., Drissi, H., Schwarz, E. M., O'Keefe, R. J., Zuscik, M. J., and Rosier, R. N. (2008) Induction of an osteoarthritis-like phenotype and degradation of phosphorylated Smad3 by Smurf2 in transgenic mice. *Arthritis Rheum.* **58,** 3132–3144
26. Li, T. F., Darowish, M., Zuscik, M. J., Chen, D., Schwarz, E. M., Rosier, R. N., Drissi, H., and O'Keefe, R. J. (2006) Smad3-deficient chondrocytes have enhanced BMP signaling and accelerated differentiation. *J. Bone Miner. Res.* **21,** 4–16
27. Bobick, B. E., and Kulyk, W. M. (2004) The MEK-ERK signaling pathway is a negative regulator of cartilage-specific gene expression in embryonic limb mesenchyme. *J. Biol. Chem.* **279,** 4588–4595
28. Gosset, M., Berenbaum, F., Thirion, S., and Jacques, C. (2008) Primary culture and phenotyping of murine chondrocytes. *Nat. Protoc.* **3,** 1253–1260
29. Alvarez, J., Sohn, P., Zeng, X., Doetschman, T., Robbins, D. J., and Serra, R. (2002) TGFβ2 mediates the effects of hedgehog on hypertrophic differentiation and PTHrP expression. *Development* **129,** 1913–1924
30. Tominaga, H., Maeda, S., Hayashi, M., Takeda, S., Akira, S., Komiya, S., Nakamura, T., Akiyama, H., and Imamura, T. (2008) CCAAT/enhancer-binding protein β promotes osteoblast differentiation by enhancing Runx2 activity with ATF4. *Mol. Biol. Cell* **19,** 5373–5386
31. Ahrens, P. B., Solursh, M., and Reiter, R. S. (1977) Stage-related capacity for limb chondrogenesis in cell culture. *Dev. Biol.* **60,** 69–82
32. Shukunami, C., Ohta, Y., Sakuda, M., and Hiraki, Y. (1998) Sequential progression of the differentiation program by bone morphogenetic protein-2 in chondrogenic cell line ATDC5. *Exp. Cell Res.* **241,** 1–11
33. Korchynskyi, O., and ten Dijke, P. (2002) Identification and functional characterization of distinct critically important bone morphogenetic protein-specific response elements in the Id1 promoter. *J. Biol. Chem.* **277,** 4883–4891
34. Canalis, E., Economides, A. N., and Gazzerro, E. (2003) Bone morphogenetic proteins, their antagonists, and the skeleton. *Endocr. Rev.* **24,** 218–235
35. Miyazono, K., Maeda, S., and Imamura, T. (2005) BMP receptor signaling. Transcriptional targets, regulation of signals, and signaling cross-talk. *Cytokine Growth Factor Rev.* **16,** 251–263
36. Stroschein, S. L., Wang, W., Zhou, S., Zhou, Q., and Luo, K. (1999) Negative feedback regulation of TGF-β signaling by the SnoN oncoprotein. *Science* **286,** 771–774
37. Sun, Y., Liu, X., Ng-Eaton, E., Lodish, H. F., and Weinberg, R. A. (1999) SnoN and Ski protooncoproteins are rapidly degraded in response to transforming growth factor β signaling. *Proc. Natl. Acad. Sci. U.S.A.* **96,** 12442–12447
38. Pearson-White, S., and Crittenden, R. (1997) Proto-oncogene Sno expression, alternative isoforms and immediate early serum response. *Nucleic Acids Res.* **25,** 2930–2937
39. Shinagawa, T., Dong, H. D., Xu, M., Maekawa, T., and Ishii, S. (2000) The *sno* gene, which encodes a component of the histone deacetylase complex, acts as a tumor suppressor in mice. *EMBO J.* **19,** 2280–2291
40. Jahchan, N. S., You, Y. H., Muller, W. J., and Luo, K. (2010) Transforming growth factor-β regulator SnoN modulates mammary gland branching morphogenesis, postlactational involution, and mammary tumorigenesis. *Cancer Res.* **70,** 4204–4213
41. Krakowski, A. R., Laboureau, J., Mauviel, A., Bissell, M. J., and Luo, K. (2005) Cytoplasmic SnoN in normal tissues and nonmalignant cells antagonizes TGF-β signaling by sequestration of the Smad proteins. *Proc. Natl. Acad. Sci. U.S.A.* **102,** 12437–12442
42. Takeda, M., Mizuide, M., Oka, M., Watabe, T., Inoue, H., Suzuki, H., Fujita, T., Imamura, T., Miyazono, K., and Miyazawa, K. (2004) Interaction with Smad4 is indispensable for suppression of BMP signaling by c-Ski. *Mol. Biol. Cell* **15,** 963–972
43. Wang, W., Mariani, F. V., Harland, R. M., and Luo, K. (2000) Ski represses bone morphogenic protein signaling in *Xenopus* and mammalian cells. *Proc. Natl. Acad. Sci. U.S.A.* **97,** 14394–14399
44. Dennler, S., Itoh, S., Vivien, D., ten Dijke, P., Huet, S., and Gauthier, J. M. (1998) Direct binding of Smad3 and Smad4 to critical TGF β-inducible elements in the promoter of human plasminogen activator inhibitor-type 1 gene. *EMBO J.* **17,** 3091–3100
45. Mankin, H. J., Dorfman, H., Lippiello, L., and Zarins, A. (1971) Biochemical and metabolic abnormalities in articular cartilage from osteo-arthritic

human hips. II. Correlation of morphology with biochemical and metabolic data. *J. Bone Joint Surg. Am.* **53,** 523–537
46. Kuroki, H., Nakagawa, Y., Mori, K., Ohba, M., Suzuki, T., Mizuno, Y., Ando, K., Takenaka, M., Ikeuchi, K., and Nakamura, T. (2004) Acoustic stiffness and change in plug cartilage over time after autologous osteochondral grafting. Correlation between ultrasound signal intensity and histological score in a rabbit model. *Arthritis Res. Ther.* **6,** R492–R504
47. Li, T. F., Gao, L., Sheu, T. J., Sampson, E. R., Flick, L. M., Konttinen, Y. T., Chen, D., Schwarz, E. M., Zuscik, M. J., Jonason, J. H., and O'Keefe, R. J. (2010) Aberrant hypertrophy in Smad3-deficient murine chondrocytes is rescued by restoring transforming growth factor β-activated kinase 1/activating transcription factor 2 signaling. A potential clinical implication for osteoarthritis. *Arthritis Rheum.* **62,** 2359–2369
48. Zhu, Q., Pearson-White, S., and Luo, K. (2005) Requirement for the SnoN oncoprotein in transforming growth factor β-induced oncogenic transformation of fibroblast cells. *Mol. Cell Biol.* **25,** 10731–10744
49. Maeda, S., Hayashi, M., Komiya, S., Imamura, T., and Miyazono, K. (2004) Endogenous TGF-β signaling suppresses maturation of osteoblastic mesenchymal cells. *EMBO J.* **23,** 552–563
50. Valdes, A. M., Spector, T. D., Tamm, A., Kisand, K., Doherty, S. A., Dennison, E. M., Mangino, M., Tamm, A., Kerna, I., Hart, D. J., Wheeler, M., Cooper, C., Lories, R. J., Arden, N. K., and Doherty, M. (2010) Genetic variation in the SMAD3 gene is associated with hip and knee osteoarthritis. *Arthritis Rheum.* **62,** 2347–2352
51. Kizawa, H., Kou, I., Iida, A., Sudo, A., Miyamoto, Y., Fukuda, A., Mabuchi, A., Kotani, A., Kawakami, A., Yamamoto, S., Uchida, A., Nakamura, K., Notoya, K., Nakamura, Y., and Ikegawa, S. (2005) An aspartic acid repeat polymorphism in asporin inhibits chondrogenesis and increases susceptibility to osteoarthritis. *Nat. Genet.* **37,** 138–144
52. Nakajima, M., Kizawa, H., Saitoh, M., Kou, I., Miyazono, K., and Ikegawa, S. (2007) Mechanisms for asporin function and regulation in articular cartilage. *J. Biol. Chem.* **282,** 32185–32192
53. Blaney Davidson, E. N., Scharstuhl, A., Vitters, E. L., van der Kraan, P. M., and van den Berg, W. B. (2005) Reduced transforming growth factor-β signaling in cartilage of old mice. Role in impaired repair capacity. *Arthritis Res. Ther.* **7,** R1338–R1347

OPEN ACCESS Freely available online

PLoS one

RBPJ Is a Novel Target for Rhabdomyosarcoma Therapy

Hiroko Nagao[1,2], Takao Setoguchi[2]*, Sho Kitamoto[3], Yasuhiro Ishidou[4], Satoshi Nagano[1], Masahiro Yokouchi[1], Masahiko Abematsu[1,2], Naoya Kawabata[1], Shingo Maeda[4], Suguru Yonezawa[3], Setsuro Komiya[1]

1 Department of Orthopaedic Surgery, Graduate School of Medical and Dental Sciences, Kagoshima University, Kagoshima, Japan, **2** The Near-Future Locomotor Organ Medicine Creation Course (Kusunoki Kai), Graduate School of Medical and Dental Sciences, Kagoshima University, Kagoshima, Japan, **3** Department of Human Pathology, Field of Oncology, Graduate School of Medical and Dental Sciences, Kagoshima University, Kagoshima, Japan, **4** Department of Medical Joint Materials, Graduate School of Medical and Dental Sciences, Kagoshima University, Kagoshima, Japan

Abstract

The Notch pathway regulates a broad spectrum of cell fate decisions and differentiation processes during fetal and postnatal development. In addition, the Notch pathway plays an important role in controlling tumorigenesis. However, the role of *RBPJ*, a transcription factor in the Notch pathway, in the development of tumors is largely unknown. In this study, we focused on the role of *RBPJ* in the pathogenesis of rhabdomyosarcoma (RMS). Our data showed that Notch pathway genes were upregulated and activated in human RMS cell lines and patient samples. Inhibition of the Notch pathway by a γ-secretase inhibitor (GSI) decreased the *in vitro* proliferation of RMS cells. Knockdown of *RBPJ* expression by RNAi inhibited the anchorage-independent growth of RMS cells and the growth of xenografts *in vivo*. Additionally, overexpression of *RBPJ* promoted the anchorage-independent growth of RMS cells. Further, we revealed that *RBPJ* regulated the cell cycle in RMS xenograft tumors and decreased proliferation. Our findings suggest that *RBPJ* regulates the RMS growth, and that the inhibition of *RBPJ* may be an effective therapeutic approach for patients with RMS.

Citation: Nagao H, Setoguchi T, Kitamoto S, Ishidou Y, Nagano S, et al. (2012) RBPJ Is a Novel Target for Rhabdomyosarcoma Therapy. PLoS ONE 7(7): e39268. doi:10.1371/journal.pone.0039268

Editor: Qiang Wang, Cedars-Sinai Medical Center, United States of America

Received March 1, 2012; **Accepted** May 22, 2012; **Published** July 9, 2012

Funding: This work was supported by Grants-in-Aid for Scientific Research (KAKENHI) (C) 19591725, (C) 20591786, (C) 21591919, (C) 21591920, (C) 22591663, (C) 24592238 and (C)23592195 and a Grant-in-Aid from the Ministry of Health, Labour, and Welfare of Japan for the Third Term Comprehensive Control Research for Cancer, and Scientific Research on Priority Areas 201201976 to HN from the Grant-in-Aid for JSPS Fellow. The funders had no role in study design, data collection and analysis, decision to publish, or preparation of the manuscript.

Competing Interests: The authors have declared that no competing interests exist.

* E-mail: setoro@m2.kufm.kagoshima-u.ac.jp

Introduction

Rhabdomyosarcoma (RMS) is the most common soft tissue sarcoma in children and adolescents [1,2,3]. Pediatric RMS can be divided into 2 major subtypes, embryonal RMS (eRMS) and alveolar RMA (aRMS). The cure rates for patients with nonmetastatic RMS have improved significantly from an estimated 25% in 1970 to 75% at present. Prognosis for RMS is dependent on the anatomic site of the primary tumor, age, completeness of resection, presence and the number of metastatic sites, and histological and biological characteristics of the tumor cells [4,5]. The advances in the understanding of tumor biology may lead to the development of novel clinically relevant therapeutic targets in the near future.

The Notch signaling cascade is highly conserved and plays a crucial role in the self-renewal of stem cells, cell fate determination, epithelial cell polarity, adhesion, cell division, and apoptosis [6,7,8]. The mammalian family of Notch receptors consists of 4 members (*NOTCH1-4*) and the ligand family consists of 5 members (*JAGGED 1/2* and *DELTA 1/3/4*). In the absence of ligand binding, the Notch receptors are inactive. Upon ligand binding, the Notch receptor is cleaved in 2 sequential steps. The cleavage events release the intracellular domain of the Notch receptor (NICD), and the NICD regulates the downstream target genes via the DNA-binding factor, *RBPJ/CBF1* [9,10]. The transcriptional regulator *RBPJ* is a highly conserved DNA-binding protein that plays a central role in canonical Notch signaling [11].

Recently, alterations in the Notch pathway have been observed in different solid tumors, including breast cancer, ovarian cancer, melanoma, glioblastoma, and lung and pancreatic cancer [12,13,14]. In addition, aberrant activation of the Notch-RBPJ pathway is involved in Epstein–Barr virus (EBV) infection [15,16], T-lymphoblastic leukemia (T-LL), and gliomas [17,18].

We previously reported that inhibition of the Notch pathway suppressed the growth of osteosarcoma by regulation of cell cycle [19]. In this study, we found that the Notch pathway was also functionally activated in human RMS, and a γ-secretase inhibitor (GSI) X reduced the *in vitro* proliferation of RMS cells. Moreover, we show that inhibition of *RBPJ* expression prevents the growth of RMS *in vitro* and *in vivo*.

Materials and Methods

Cell Lines

RD and KYM-1 cell lines were obtained from the Health Science Research Resources Bank (HSRRB, Osaka, Japan). RMS-YM cell line was obtained from Riken Bioresource Center (Tsukuba, Japan). HSKMc cell line was purchased from TOYOBO (Osaka, Japan). RD and KYM-1 cell lines were cultured in Dulbecco's modified Eagle's medium (DMEM)

supplemented with 10% fetal bovine serum (FBS), 100 U/mL penicillin, and 100 μg/mL streptomycin. RMS-YM cell line was cultured in RPMI 1640 medium supplemented with 10% FBS, 100 μM nonessential amino acids (NEAA), 20 mM HEPES, 100 U/mL penicillin, and 100 μg/mL streptomycin. HSKMc cell line was cultured in skeletal muscle cell growth medium (TOYOBO, Osaka, Japan). All cells were maintained at 37°C in 5% CO_2.

Patient Specimens

Human eRMS biopsy specimens were collected from primary lesions before any diagnostic or therapeutic treatment. Human skeletal muscle tissues were collected from patients undergoing operation for scoliosis. The study protocol was approved by the institutional Review Board of Kagoshima University. Informed consent was obtained from all patients.

Real-time PCR Analysis

Real-time PCR analysis was performed as previously described [20]. Total RNA was extracted from cell lines and tissue specimens using miR-Vana RNA isolation kit or TRIzol (Invitrogen, CA, USA) and was reverse transcribed using ReverTra Ace -α- (TOYOBO, Osaka, Japan). cDNA was amplified by real-time PCR using SYBR Green (Life Technologies, NY, USA). Real-time PCR was performed on MiniOpticon^{TM} (Bio-Rad, Tokyo, Japan). The comparative Ct (ΔΔCt) analysis was performed to evaluate the fold change of mRNA expression, using the expression of *ACTB* as a reference. All PCR reactions were performed in triplicate. All primers were designed. using Primer 3 software. The following primers were used: *ACTB*, 5′-AGAAAATCTGGCACCACACC-3′ and 5-AGAGGCGTACAGGGATAGCA-3′; *NOTCH1*, 5′-GTGACTGCTCCCTCAACTTCAAT-3′ and 5′-CTGTCACAGTGGCCGTCACT-3′; *NOTCH2*, 5′-GTGTCAGAATGGAGGGGTTTG-3′ and 5′-ATTGCGGTTGGCACAGG-3′; *NOTCH3*, 5′-CAACCCGGTGTACGAGAAGT-3′ and 5′-GAACGCAGTAGCTCCTCTGG-3′; *NOTCH4*, 5′-CCATTGACACCCAGCTTCTT-3′ and 5-GCTGAACAGAAGTCCCGAAG-3′; *JAG1*, 5′-CAGATTTCCTTGTTCCCTTGCT-3′ and 5′-CGTTGTTGGTGGTGTTGTCC-3′; *DLL1*, 5′-CCTACTGCACAGAGCCGATCT-3′ and 5′-GCAGGTGGCTCCATTCTTGC-3′; *HES1*, 5′-AGGCGGACATTCTGGAAATG-3′ and 5′-CGGTACTTCCCCAGCACACTT-3′; *HEY1*, 5′-CGAGGTGGAGAAGGAGAGTG-3′ and 5′-CTGGGTACCAGCCTTCTCAG-3′; *RBPJ*, 5′-CGCATTATTGGATGCAGATG-3′ and 5′-CAGGAAGCGCCATCATTTAT-3′; *Cyclin D*, 5′-CAGAAGTGCGAGGAGGAGGT-3′, and 5′-CGGATGGAGTTGTCGGTGT-3′; *Cyclin E*, 5′-CCACACCTGACAAAGAAGATGATGAC-3′ and 5′-GAGCCTCTGGATGGTGCAATAAT-3′; *E2F1*, 5′-ATGTTTTCCTGTGCCCTGAG-3′ and 5′-ATCTGTGGTGAGGGATGAGG-3′; *SKP2*, 5′-TGGGAATCTTTTCCTGTCTG-3′ and 5′-GAACACTGAGACAGTATGCC-3′; *p21*, 5′-GACACCACTGGAGGGTGACT-3′ and 5′-ACAGGTCCACATGGTCTTCC-3′.

Cell Proliferation Assay

Cell proliferation assay was performed as previously described [21]. We seeded 1×10^3 cells (RD) or 3×10^3 cells (KYM-1)/100 μL in a 96 -well plate. Next day, the cells were placed in fresh medium containing the indicated concentration of the GSI X (CALBIOCHEM, Basel, Switzerland), GSI XX (CALBIOCHEM, Basel, Switzerland) or DMSO and were cultured for 3–4 days. Cell growth were measured daily by performing WST-1 assay (Roche, Basel, Switzerland).

Plasmid Constructs and Gene Transfer

Control siRNA (S20C-0600) was purchased from B-Bridge International (Cupertino, USA) and RBPJ siRNA (sc-38214) was purchased from Santa Cruz Biotechnology (CA, USA). All siRNA transfection experiments were performed using Lipofectamine RNAiMAX (Invitrogen, CA, USA) transfection reagent according to the manufacturer's protocol. Control or RBPJ shRNA (KH06319P) were purchased from SuperArray Biosciences (MD, USA). pCMV6-Entry Vector (PS100001) and RBPJ expression vector (RC204791) were purchased from Origene (Maryland, USA). All plasmid transfection experiments were performed using FuGENE6 (Roche, Basal, Switzerland) transfection reagent according to the manufacturer's protocol. Tranfected cells were selected in 700 μg/mL neomycin or 0.4 ng/μL puromycin. Stable cell lines were then used for colony formation assay and in vivo experiments.

Colony Formation Assay

Colony formation assay was performed as previously described [22]. Cells were suspended in DMEM containing 0.33% soft agar and 5% FBS and then were plated on a 0.5% soft agar layer. Cells were cultured at a density of 2×10^4 cells per well in 6-well plates. After 2–3 weeks (RBPJ siRNA/RD: 2 weeks, RBPJ/RD: 3 weeks), the number of colonies was counted. Every experiment was performed in triplicate, and all experiments were performed 3 times.

Western Blotting Analysis

Western blotting analysis was performed as previously described [23].

Cells were lysed using NP40 buffer, including 0.5% NP40, 10 mM Tris-HCl (pH 7.4), 150 mM NaCl, 3 mM pAPMSF (Wako Chemicals, Kanagawa, Japan), 5 mg/mL aprotinin (Sigma, StLouis, USA), 2 mM sodium orthovanadate (Wako Chemicals, Kanagawa, Japan), and 5 mM EDTA. Lysates were boiled with sodium dodecyl sulfate (SDS) sample buffer, separated by SDS-polyacrylamide gel electrophoresis (PAGE) (Bio-Rad, Tokyo, Japan), and transferred to a polyvinylidene fluoride (PVDF) membrane (Caliper LifeSciences, CA, USA). The membranes were blocked in 5% nonfat dry milk TBST buffer and incubated in primary antibodies diluted in TBST for 1 h at room temperature or overnight at 4°C. Blots were washed using TBST buffer and incubated with horseradish peroxidase-conjugated secondary antibodies (Cell Signaling Technology) in TBST buffer for 45 min at room temperature. Immunocomplexes were visualized using an enhanced chemiluminescence kit (GE Healthcare, Tokyo, Japan). Primary antibodies were RBPJ (1:300, ab33065, abcam), PARP (1:1000, #9542, Cell Signaling) and α-tubulin (1:1000, DM1A, Sigma-Aldrich).

Animal Studies

Xenograft experiments were performed as previously described [24]. Briefly, control or RBPJ shRNA-transfected RD cells (1×10^6) were suspended in 100 μL Matrigel (BD, NJ, USA). Cell suspensions were subcutaneously inoculated in 5-week-old nude mice (Japan SLC, Inc). Tumor size was calculated weekly using the formula $LW^2/2$ (with L and W representing the length and width of tumors). Kaplan–Meier analysis was performed using Kaplan 97 software. All animal experiments were performed in compliance with the guidelines and approved by the Animal